Journal of Environmental Radioactivity 276 (2024) 107446

Contents lists available at ScienceDirect

Journal of Environmental Radioactivity

journal homepage: www.elsevier.com/locate/jenvrad

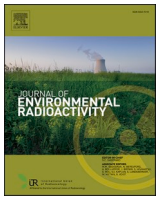

Review

Parameter uncertainty analysis of the equivalent lung dose coefficient for the intake of radon in mines: A review

Thomas Makumbi [a,*], Bastian Breustedt [b], Wolfgang Raskob [a]

[a] Institute for Thermal Energy Technology and Safety, Karlsruhe Institute of Technology, Hermann-von-Helmholtz Platz 1, 76344, Eggenstein-Leopoldshafen, Germany
[b] Institute of Biomedical Engineering, Karlsruhe Institute of Technology, Fritz-Haber-Weg 1, D-76131, Karlsruhe, Germany

ARTICLE INFO

Keywords:
Radon
Progeny
Uncertainty
Mines
Lung
Dose

ABSTRACT

Radon presents significant health risks due to its short-lived progeny. The evaluation of the equivalent lung dose coefficient is crucial for assessing the potential health effects of radon exposure. This review focuses on the uncertainty analysis of the parameters associated with the calculation of the equivalent lung dose coefficient attributed to radon inhalation in mines. This analysis is complex due to various factors, such as geological conditions, ventilation rates, and occupational practices. The literature review systematically examines the sources of radon and its health effects among underground miners. It also discusses the human respiratory tract model used to calculate the equivalent lung dose coefficient and the associated parameters leading to uncertainties in the calculated lung dose. Additionally, the review covers the different methodologies employed for uncertainty quantification and their implications on dose assessment. The text discusses challenges and limitations in current research practices and provides recommendations for future studies. Accurate risk assessment and effective safety measures in mining environments require understanding and mitigating parameter uncertainties.

1. Introduction

Radon is a naturally occurring radioactive noble element that occurs as a gas or is usually dissolved in water (Sakoda et al., 2021). The element radon occurs naturally in three isotopes, i.e., radon (Rn-222), thoron (Rn-220) and actinon (Rn-219); these isotopes are usually found as progeny radionuclides of radium isotopes (Ra-226, Ra-224 and Ra-223) in the natural radioactive decay chains of U-238, Th-232 and U-235 respectively in the Earth's crust (Abdo et al., 2021). Rn-222, with a half-life of 3.82 days, is the most abundant of these isotopes in nature due to its relatively long half-life and can be found in rocks and soils of different environments such as uranium and coal mines, caves, metro stations and tunnels, underground car parks, spas and wine cellars of houses (Carillo et al., 2015; Abdo et al., 2021).

Rn-222 gas emanates from the Earth's crust and can leave the ground and enter the atmosphere by convection and diffusion, and is therefore present in indoor and outdoor air (Brudecki et al., 2014; Mirsch et al., 2020). Unlike Rn-222, Rn-220 has a shorter half-life (56 s) and travels shorter distances from its point of origin than Rn-222. As a result, building materials are the main source of indoor exposure to Rn-220. As Rn-219 has the shortest half-life (4 s), it is generally less able to escape from the source. As a result, workplace exposures to Rn-219 and its progeny are generally low and negligible. Consequently, Rn-222 and Rn-220 are the most important radon isotopes in radiation protection; in recent decades it has been recognized that exposure to these isotopes is the single largest contributor to natural radiation exposure in humans (Mirsch et al., 2020; Wang et al., 2021).

Inhalation of Rn-222 and its progeny is a leading cause of lung cancer among underground miners and indoor workers, and the second leading cause of lung cancer worldwide after tobacco smoking (Bi et al., 2010; Hu et al., 2020; Chen 2023; Skubacz et al., 2023), with the lung being the organ that receives the largest dose; almost all of the dose (>95%) comes from inhalation of the progeny rather than from the gas itself, as almost all of the inhaled gas is subsequently exhaled (Harrison and Marsh, 2012; Hu et al., 2022). However, a large proportion of inhaled radon progeny is deposited in the respiratory tract of the lung and, because of its short half-life, delivers a large proportion of the dose to the lung tissue before being cleared either by absorption into blood or by particle transport to the digestive tract (Papenfuβ et al., 2023). Two of the short-lived radon progenies (Po-218 and Po-214) decay by alpha

* Corresponding author.
E-mail address: thomas.makumbi@kit.edu (T. Makumbi).

https://doi.org/10.1016/j.jenvrad.2024.107446
Received 16 January 2024; Received in revised form 14 April 2024; Accepted 3 May 2024
Available online 11 May 2024

emission, and it is the energy of these alpha particles that accounts for most of the dose to lung tissue (Romano et al., 2019). The equivalent dose to the lung following inhalation of radon and its short-lived progeny can be calculated using the Human Respiratory Tract Model (HRTM) developed by the International Commission for Radiological Protection (ICRP).

One of the main challenges in assessing the equivalent lung dose for radon progeny intake is that the ICRP models are reference models with parameters representative of a reference person; by definition, the model parameters are fixed values without uncertainty (Paquet et al., 2016). Therefore, sensitivity analysis and estimation of the associated parameter uncertainties in HRTM need to be performed to better understand the models and estimate the influence of individual parameters on the model predictions (Breustedt et al., 2017, 2018). Therefore, consideration of parameter uncertainties provides a basis for risk assessment of exposure to radon progeny. Secondly, uncertainty analysis provides a means of identifying the important pathways in effective dose calculation and assessing its reliability as a radiation protection quantity (Puncher and Harrison, 2012b). Therefore, the results of such a study can provide information on the reliability of the assessed doses and point to sensitive parameters for a better fit of the models to the monitoring data.

The aim of this review is therefore to identify the parameters that affect the calculated lung dose per unit exposure to radon progeny in underground mines and their respective probability distributions, which can be used as a guide in future studies by the authors and other stakeholders. The authors intend to use this information in their uncertainty studies in underground uranium mines for the two exposure scenarios of wet drilling with good ventilation and dry drilling with poor ventilation. More information on these scenarios is presented in section 7 of this paper.

This paper is structured as follows: Section 2 describes the sources of radon in underground mines and the factors that influence its movement from the source into enclosed spaces; this section also looks at the potential health effects of radon on humans. Section 3 discusses the HRTM. This section describes the morphology, deposition and particle transport and dissolution/absorption components of the HRTM. Section 4 describes the equivalent lung dose coefficient and its relevance to the assessment of radiation risk to underground miners. Section 5 discusses the sources of uncertainty and variability in the HRTM and how they affect the calculation of the equivalent lung dose coefficient. Section 6 describes the methods used to quantify uncertainties in internal dosimetry. Section 7 discusses the parameters that affect the calculated equivalent lung dose coefficient from uptake of radon progeny by underground miners for the two exposure scenarios of interest to the authors, and presents their respective probability distributions. Section 8 discusses the challenges and limitations in assessing the uncertainties in the equivalent lung dose coefficient for intake of radon and progeny in underground mines. Section 9 discusses how the results of the various studies in the literature compare. Section 10 discusses the regulatory implications for radon exposure in underground mines. Finally, Section 11 summarizes the results of the review and their implications for future research.

2. Radon in mines: sources and health impacts

2.1. Sources of radon

The prevailing geology determines the radon concentration in an area. Relatively high levels of radon are associated with certain types of bedrock and unconsolidated deposits. Soil radon concentrations within a few meters of the ground surface are most important in determining radon release rates into pore spaces and subsequently into the atmosphere. These depend on the distribution and concentration of the parent radium radionuclides in the bedrock and overburden and on the permeability of the soil. Some generalizations can be made about radium concentrations in different types of rock, but there is a very wide range within each type. In general, granites have relatively high levels of radium, sedimentary and metamorphic rocks have intermediate levels, and basalts and most limestones have low levels, although there are many striking exceptions to this rule. Soils are similarly variable in radium content and generalizations are even more difficult. This is partly due to the often-complex relationship between the bedrock and its overburden, particularly in those higher latitude regions that have been subject to glaciation in the past (UNSCEAR, 2000).

Radium is more readily transferred to vegetation than the parent uranium radionuclides, and emission from soil organic matter is more effective than from soil minerals. The effective permeability of bedrock and soils is also highly variable and is related to the degree of weathering, porosity, moisture content and the presence of fractures or fissures. Schumman and Gundersen (1996) showed that regional differences can be attributed to climate-related differences in soil weathering processes, with the key parameters characterizing radon transport being the radon diffusion coefficient and soil-air permeability. Radon isotopes can enter underground environments, such as mines, in a number of ways, including emanation from the host rock and dissolution from mine/groundwater (Kleinschmidt et al., 2018).

According to the ICRP (2017), uranium, radium and thorium occur naturally in soil and rocks and can be a continuous source of radon. Radon gas can escape from the Earth's crust by molecular diffusion or convection and is present in both indoor and outdoor air; the accumulation of radon in enclosed spaces is what creates the radiation hazard. This applies to certain working environments such as underground mines, tourist caves and underground water systems. Radon can diffuse in soil more than 1 m from its point of origin. Therefore, the soil beneath buildings is usually the main source of indoor radon.

2.2. Health impacts of radon

Studies conducted by epidemiologists show that miners exposed to high levels of radon for long periods of time have an increased risk of lung cancer, and that the incidence of lung cancer increases significantly with increasing exposure to radon and its progeny (Kleinschmidt et al., 2018; Hu et al., 2022). High levels of radon can induce more changes in the blood cells of the body than low to moderate levels (Liu et al., 2022). Liu et al. (2022) also claim that radon exposure can increase chromosomal aberrations in human peripheral blood lymphocytes, in addition to the effects of other factors such as cigarette smoke, dust and exhaust fumes. The risk of lung cancer from radon in miners is further increased by tobacco smoking. Bersimbaev and Bulgakova (2015) argue that tobacco smoking can increase the oncogenic effect of radon by a factor of 2–10, and that radon exposure can significantly reduce the latency period of lung cancer.

Additional health risks from radon have been reported in literature (Khursheed, 2000; Kendall and Smith, 2002; Hussein 2008). Hussein (2008) reported that inhaled radon progeny can escape from the lungs to systemic organs and tissues and cause kidney and prostate cancer. Hussein (2008) further asserts that there is a positive correlation between radon exposure and coronary heart disease, as evidenced by an increased risk of coronary heart disease mortality observed in miners with accumulated radon exposures in excess of 1000 working level months (WLM), where WLM is defined as the cumulative exposure from breathing an atmosphere at a concentration of 1 working level (WL) for a working month of 170 h; WL refers to any combination of the short-lived radon progeny in 1 m^3 of air that results in the emission of 1.3E+08 MeV alpha energy (ICRP, 2017).

Further epidemiological studies conducted in the Czech Republic indicated an association between radon exposure and the incidence of chronic lymphocytic leukemia (Rericha et al., 2006). However, this finding could not be confirmed by results from similar studies in the Czech Republic and Germany (Tomasek and Malatova, 2006; Möhner et al., 2006, 2010). Radon has also been associated with melanoma and

childhood cancer (Evrard et al., 2006; Raaschou-Nielsen, 2008), although this finding was not supported by results from several case-control studies (Lubin et al., 1998; Steinbuch et al., 1999).

Bersimbaev and Bulgakova (2015) also reported an increase in malignant tumors of the liver, stomach and breast over the past 35 years among uranium miners in eastern Kazakhstan, while other researchers have linked radon progeny to skin cancer risk (Kleinschmidt et al., 2018; Sakoda et al., 2021; Hofmann et al., 2021). Finally, ingestion of radon in drinking water is associated with stomach cancer, although the risk is considered to be extremely low when compared to that from inhalation (Kendall and Smith, 2002; Bersimbaev and Bulgakova, 2015).

In conclusion, exposure to radon progeny in mines has been associated with cancer incidence, although the available epidemiological evidence is inconsistent to draw firm conclusions about the association between radon exposure and cancers other than lung cancer.

3. The human respiratory tract model (HRTM)

The ICRP HRTM describes the deposition, clearance and dosimetry of inhaled material in the lung and is used to calculate dose coefficients for workers and the public for inhalation intakes (ICRP, 1994; Puncher et al., 2008). The model provides a suitable compromise between physiological realism and ease of practical application, so that in addition to its use in radiation protection, it has been used to calculate lung doses in epidemiological studies of nuclear workers exposed to plutonium and other actinides (Bailey and Puncher, 2007). However, the emergence of new experimental data and a review of existing data prompted an update of the HRTM. The changes were applied to the compartments representing particle transport from the bronchial (BB), bronchiolar (bb) and alveolar-interstitial (AI) regions of the lung and deposition and clearance from the extrathoracic (ET) region (Puncher et al., 2013). The HRTM consists of the deposition model, the clearance model and the particle dissolution/absorption model. For more detailed information on the HRTM, the interested reader is referred to ICRP publications 66 and 130 (ICRP, 1994, 2015).

3.1. Morphometry

The HRTM model is divided into two main parts. The first part represents the extrathoracic (ET) region, which consists of the anterior nasal passages (ET_1) and the posterior nasal passages (ET_2), i.e., the larynx, pharynx and mouth. The second part represents the thoracic (TH) region, which includes the bronchial region (BB), i.e., airway generations 0–8, the bronchiolar region (bb), i.e., airway generations 9–15, and the alveolar interstitial region (AI), which comprises the first respiratory bronchioles through the alveolar sacs and includes interstitial connective tissues, i.e., from generation 16 (ICRP, 2015). Lymph nodes are associated with both the ET and TH regions (LN_{ET} and LN_{TH}, respectively). Target cells are identified in each region, e.g., basal cells of the epithelium in both ET regions, basal and secretory cells in the bronchial epithelium and secretory cells in the bronchiolar epithelium. Reference values for dimensions that define the mass of tissue containing target cells in each region for dose calculations are provided and are assumed to be independent of age and sex (ICRP, 1994, 2015; Bailey and Puncher, 2007).

3.2. Physiology

The primary respiratory parameters are ventilation rate, B (m^3/h), respiratory frequency, f_R (breaths per minute) and tidal volume, V_T (liters). These HRTM parameters are dependent on the subject's age and level of physical activity (Bailey and Puncher, 2007; Puncher et al., 2008). Other physiological parameters include the distribution of inhaled air between the nose and mouth, F_n and breathing mode. ICRP (1994) provides reference values for these parameters in addition to the four activity levels of a worker, i.e., sleep, sitting, light and heavy physical activity. These, combined with the habit survey data, give the reference quantities inhaled by a worker per shift or per day. For radon progeny dosimetry, these parameters can also determine intakes per unit exposure to radon progeny (Marsh et al., 2012).

3.3. Particle deposition

Deposition of particles in the respiratory tract depends on the physical properties of the aerosols (i.e., mean size and size distribution, density and shape factor) as well as subject parameters (i.e., breathing mode, ventilation rate and age). In terms of physical properties, deposition is particularly influenced by particle size, with large particles represented by their activity median aerodynamic diameter (AMAD) and smaller particles represented by their activity median thermodynamic diameter (AMTD). The AMAD is used to characterize aerosols whose deposition is dominated by sedimentation and inertial impaction mechanisms, i.e., 50% of the activity is characterized by an equivalent aerodynamic diameter (d_{ae}) greater than the AMAD, where d_{ae} is defined as the diameter of a sphere of unit density having the same settling velocity in air as the particle of interest (Bolch et al., 2001). Sedimentation and impaction are aerodynamic effects that are important for particle sizes above 0.1 μm and increase with size (Bailey and Puncher, 2007).

When diffusion (Brownian motion) dominates particle deposition, the aerosol is characterized by an AMTD, i.e., 50% of the activity is associated with particles larger than the AMTD. Particle behavior can be described by the thermodynamic equivalent diameter (d_{th}), which is defined as the diameter of a spherical particle with the same diffusion coefficient in air as the particle of interest (Bolch et al., 2001). Diffusion is a thermodynamic effect that is important for particle sizes below 0.1 μm and increases with decreasing size (Bailey and Puncher, 2007).

The HRTM deposition model evaluates the fraction of activity in the inhaled air that is deposited in each region of the airways, and the regions are treated as a series of successive filters during both inhalation and exhalation, the efficiency of each being determined by considering aerodynamic and thermodynamic processes acting in competition (ICRP, 1994).

Two additional aerosol parameters are of interest for radon progeny, namely the equilibrium factor (F), a measure of the relationship between radon gas activity and its progeny, and the unattached fraction (f_p), which gives the fraction of radon progeny that is not attached to atmospheric aerosols. The particles to which radon progeny are attached can have a trimodal size distribution, i.e., nucleation mode (ultrafine particles nucleated by condensation processes and chemical reactions), accumulation mode (fine particles accumulated by various processes) and coarse mode (coarse particles that can be produced mainly by mechanical processes), with only the accumulation mode assumed for mines (ICRP, 2017; Hu et al., 2020). Inhalation is assumed to lead to hygroscopic growth, so that the attached particles increase by a factor of 2 in the respiratory tract upon inhalation. This is represented by the hygroscopic growth factor (Marsh et al., 2008, 2012; Hu et al., 2020).

When gases are inhaled, deposition depends on the chemical properties rather than the physical properties of the inhaled gas (ICRP, 2015). However, this is not the case for a noble gas such as radon, where no deposition occurs. For the inhalation of radon gas, the activity concentration in the inhaled air is assumed to be in equilibrium with that in the ambient air (ICRP, 2017). Leggett et al. (2013) showed that inhaled radon gas is partially absorbed into the arterial blood and transported to other parts of the body, from where it is then transported back to the respiratory tract via the venous blood, where it is partially exhaled and partially reabsorbed back into the arterial blood, and the cycle continues until the body burden is depleted by exchange between pulmonary blood and respiratory air and loss from the body in the exhaled air.

3.4. Particle transport

The model structure and the values of the model parameters representing or describing physiological processes are typically assumed to be the same for all elements, although the latter are expected to vary between individuals in a population. According to ICRP (2015), mechanical processes remove the deposited material from ET_1, which has a biological half-life of 8 h. Approximately two-thirds are transferred to ET_2, with the remaining fraction released to the environment by extrinsic means such as sneezing and nasal wiping (ICRP, 2015; Hu et al., 2020).

Mucociliary clearance transports deposited material from all regions of the airways to ET_2, from where it is transported to the digestive tract with a biological half-time of 10 min. However, this mucociliary clearance is slower in the lower lung region than in the upper lung region. The biological half-times are 230 days from AI to bb, 3.5 days from bb to BB and 1.7 h from BB to ET_2. Mechanical transport to the regional lymph nodes also occurs from all regions except ET_1. With the exception of the AI region, 0.2% of the deposited material is assumed to be transported to the lymph nodes with a biological half-life of 1.9 years. Within the AI region, the model assumes that one third of the deposited material is transported to the lymph nodes with a biological half-time of more than 600 years (ICRP, 2015).

3.5. Dissolution and absorption

The HRTM uses a simple compartmental model to represent time-dependent dissolution, in which the absorption of material deposited in ET_2 and the thoracic airways into the blood is assumed to occur by a two-step process, i.e., dissolution of the inhaled material, described by three parameters: the fraction of material that dissolves rapidly f_r, the dissolution rate for the rapid fraction s_r, and the dissolution rate of the remaining fraction ($1\text{-}f_r$) at a rate s_s (ICRP, 2015).

The values of the dissolution parameters are assumed to be determined by the physicochemical properties of the inhaled material and thus its chemical form (Hu et al., 2020). Dissolution is then followed by uptake of the dissolved material into blood, a process which is assumed to be instantaneous unless the dissolved ions of the radionuclide become bound to the airway walls. The fraction of material that becomes bound after dissolution is represented by the bound fraction f_b. Since the ionic form of the radionuclide determines the extent of any bound state, it is assumed to be independent of the chemical form of the inhaled radionuclide. The uptake of material into blood from the bound state is assumed to occur at a rate s_b (Puncher and Burt, 2013; Puncher 2014a, 2014b).

Absorption into the blood from each region of the respiratory tract except ET_1, where no absorption is assumed, occurs at the same transfer rate, generally with a fast and a slow component. As absorption rates depend on the solubility of the substance, ICRP has defined default rates F, M and S for fast, moderate and slow absorption, respectively, in addition to providing compound-specific parameters where relevant data are available (ICRP, 2015).

3.6. Dosimetry

For dosimetric purposes, the thoracic airways are divided into three regions, i.e., BB, bb and AI; lymphatic nodes are also associated with the thoracic airways, but the dose to the lymphatic nodes can be ignored for radon progeny, as almost all progeny will have decayed before reaching the lymphatic nodes (Marsh et al., 2008). The radiosensitive target cells identified in the thoracic region include basal and secretory cells in the bronchial epithelium; Clara cells (a type of secretory cell) in the bronchiolar epithelium; and endothelial cells such as those of capillary walls and type II epithelial cells in the AI region.

The definition of the radiosensitive cells for which dose values are calculated and their depth within the tissue are of key importance for the dose received from alpha radiation. According to ICRP (2015), radiosensitive cells are distributed throughout the AI region and regional lymph nodes, while in other areas they are assumed to be in a tissue layer at a certain depth within the airways. In the ET region these cell layers are assumed to be the basal cells at a depth of 40–50 μm, in the BB region they are assumed to be the secretory cells (10–40 μm) and the basal cells (35–50 μm) and in the bb region they are assumed to be the secretory cells (4–12 μm). The dose to the BB region is calculated as the arithmetic mean of the dose values for the secretory and basal cells; the dose to the ET region is calculated as the weighted average of the dose values for the nasal passage (ET_1: 0.001) and the oral cavity/larynx (ET_2: 0.999), while the lung dose is calculated as the arithmetic sum of the dose values for the BB, bb and AI regions. The dose to the LN_{TH} and LN_{ET} is included in the dose calculation for the lymphatic tissue (0.08 each).

The effective dose from radon inhalation is determined in particular by the lung dose received from alpha radiation. This means that the radiation and tissue weighting factors are applied directly. The tissue weighting factor of 0.12 is used for the lung and a radiation weighting factor for alpha radiation of 20 is applied (Hu et al., 2020).

4. Equivalent lung dose coefficient: definition and its significance

The equivalent lung dose coefficient gives the dose (Sv) to the lung per unit activity intake (Bq) and has the units Sv/Bq. The deposition and clearance models of the HRTM make it possible to calculate the amounts of activity and the number of decays in the various regions of the respiratory tract at any time after intake. The dosimetric model, on the other hand, allows the calculation of the resulting doses to each region of the lung (ICRP 1994, 2015).

The equivalent lung dose per unit exposure to short-lived radon progeny is calculated in terms of Sv per potential alpha energy exposure (in units of Sv/WLM or Sv/Jhm^{-3}). The radon progeny activity intake, I_i (Bq), for a subject exposed to 1 WLM is given by Eq. (1) from ICRP Publication 137 (ICRP, 2017).

$$I_i = C_i.B.t \quad (1)$$

where;

- C_i is the activity concentration of radon progeny i corresponding to a radon progeny mixture of 1 WL (Bq/m^3).
- B is the average breathing rate of the reference worker i.e., adult male performing light work (m^3/h).
- t is the exposure period of 170 (h) derived from the definition of WLM.

The effective dose per unit exposure from the inhalation of short-lived radon progeny is calculated by combining the intakes (I_i) with the effective dose coefficients for the individual radon progeny using Eq. (2), also taken from ICRP Publication 137 (ICRP, 2017).

$$E = \sum_j f_{p,j} \sum_{i=1}^{3} I_{j,i}.e_{j,i} \quad (2)$$

where;

- E is the effective dose per unit exposure to radon progeny (Sv/WLM),
- j corresponds to the aerosol mode of the activity size distribution, i.e., j = 1, 2 and 3 for the unattached, nucleation and accumulation modes respectively.
- i = 1, 2 and 3 corresponds to the inhaled short-lived radon progeny, i.e. Po-218, Pb-214 and Bi-214 respectively.
- $e_{j,i}$ is the effective dose coefficient (Sv/Bq) for inhalation of progeny i with an activity size distribution for mode j.

- $f_{p,j}$ is the unattached fraction for mode j.

The activity concentration (Table 1) of radon progeny varies with the environmental conditions of exposure. However, Marsh and Birchall (2000) showed that for intakes of short-lived radon progeny, the equivalent lung dose per unit exposure is relatively insensitive to F. This is because WL is defined in terms of potential alpha energy concentration (PAEC) and the fraction of alpha energy absorbed by target tissues in the lung is similar for Po-218 and Po-214 per decay. For dosimetry purposes, the following activity ratios can be assumed (ICRP, 2017);

Unattached: Po-218: Pb-214: Bi-214 = 1:0.1:0

Attached: Po-218: Pb-214: Bi-214 = 1:0.75:0.6

5. Uncertainty, variability and factors contributing to parameter uncertainty

Uncertainty refers to a lack of knowledge about a particular parameter value, where the value itself is fixed but not known with precision (Puncher and Burt, 2013). Uncertainty is expressed as a probability in Bayesian inference or as a confidence interval in classical statistics (Puncher and Harrison, 2012a). Variability, on the other hand, refers to the natural range and frequency that a parameter value can assume in individuals within a population of interest. Variability and uncertainty are sometimes referred to as aleatory and epistemic uncertainty, respectively (Puncher and Harrison, 2012b; Li et al., 2015; Paquet et al., 2016).

The variability of biokinetics within a population is often an important factor contributing to the uncertainty in a central estimate of a biokinetic quantity. This is because such variability contributes to the problem of identifying the central tendency of these properties in the population, due to the small number of observations generally available and also because subjects in biokinetic studies are often not randomly selected. According to Paquet et al. (2016), variability in the biokinetics of radionuclides, drugs or chemicals in humans is due to many physiological factors or modulating effects of an environmental nature, such as age, sex, pregnancy, lactation, exercise, disease, stress, smoking and diet.

It is important to distinguish between uncertainty and variability, or more correctly, to consider variability as a component of uncertainty in certain cases (Puncher and Harrison, 2012b). Harrison and Day (2008) argue that while uncertainty refers to the degree of confidence that can be placed in given parameter values or dose estimates as central values for a population, variability, in the limited sense of dose and risk assessment, refers to quantitative differences between different members of the population in question and in this limited sense is biological variability. It can therefore be concluded that uncertainty affects the distribution of the mean, whereas variability should only affect its location. It is therefore important that the different effects of uncertainty and variability are taken into account in an uncertainty analysis if the aim is to determine the uncertainty in the population mean dose or cancer risk resulting from the intake of a radionuclide.

The uncertainty in an internal dose assessment based on bioassay data depends on several factors, such as the uncertainties associated with the measurements used to determine the activity of a radionuclide in vivo or in a biological sample, uncertainties in the exposure scenario used to interpret the bioassay results, and uncertainties in the biokinetic and dosimetric models used to interpret the bioassay results (Harrison et al., 2001; Paquet et al., 2016). Some uncertainties due to measurement techniques and subjective behavior can be reduced, while those due to natural human variability can be quantified but are difficult to reduce.

Paquet et al. (2016) reported that the ICRP has made considerable efforts to revise and improve its models to make them more physiologically realistic. As a result, the ICRP models are now sufficiently sophisticated to be used in the calculation of absorbed doses to organs and tissues for scientific purposes and in many other fields such as toxicology, pharmacology and medicine. Several authors have presented the sources and levels of uncertainty in internal dosimetry (Leggett, 2001, 2003; Harrison et al., 2001; Leggett et al., 2007; Paquet et al., 2016; ICRP, 2017; Li, 2018; Breustedt et al., 2018; Kwon et al., 2020). The main factors identified by these authors are outlined below;

Uncertainties in the exposure scenario: These include the uncertainty in (i) the time and route of intake, (ii) the uncertainty in the particle size distribution of the inhaled radionuclide aerosols, (iii) the uncertainty in the physicochemical form of the inhaled radionuclide and (iv) the influence of background radiation.

Uncertainties in biokinetic models: These include (i) uncertainties in the structure of a biokinetic model, (ii) uncertainties due to the type of information used to construct biokinetic models, (iii) uncertainties associated with the application of human data, (iv) uncertainties in interspecies extrapolation of biokinetic data, (v) uncertainties due to inter-element extrapolation of biokinetic data, and (vi) uncertainties in central estimates due to within-population variability.

Uncertainties in dosimetric models: These include (i) the energy and intensity of the nuclear and atomic radiation emitted by the radionuclide and any radioactive progeny, (ii) the interaction coefficients of the emitted radiation in tissues, (iii) the elemental composition of body tissues, (iv) the geometry and density of body organs, and (v) parameters describing the spatial relationship between the source and target regions.

Table 1
Activity concentration of a mixture of short-lived radon progeny or thoron progeny that give 1 WL for either unattached or attached progeny (ICRP, 2017).

Nuclide	Activity concentration (Bq/m^3)	
	Unattached	Attached[a]
Rn-222 progeny[b]		
Po-218	2.41E4	5.21E3
Pb-214	2.41E3	3.91E3
Bi-214	0	3.13E3
Rn-220 progeny[c]		
Pb-212	3.01E2	2.94E2
Bi-212	0	7.36E1

[a] It is assumed that the activity concentrations of radon progeny for each of the attached modes are the same.
[b] Activity ratios of Po-218: Pb-214: Bi-214 are assumed for the unattached and attached modes respectively.
[c] Activity ratios of Pb-212: Bi-212 of 1.0:0 and 1.0:0.25 are assumed for the unattached and attached thoron progeny modes respectively.

6. Methodologies for parameter uncertainty analysis

6.1. Monte Carlo methods

Monte Carlo methods are used to find solutions to mathematical and statistical problems by simulation (Everitt, 1995). In a Monte Carlo analysis, a value is randomly drawn from the distribution of each input. Together, this set of random variables defines a scenario which is used as inputs to the model and the outputs of the model are then calculated (Morgan and Henrion, 1990). The resulting simulated distribution of outputs is used to assess the uncertainty introduced by the input uncertainty. Monte Carlo simulations can also be used in a sensitivity analysis to identify important input parameters.

With the advent of more powerful and inexpensive computers, Monte Carlo methods are probably the most commonly used methods for uncertainty analysis today. Monte Carlo methods often use simple random sampling, but can also use more sophisticated sampling methods for greater efficiency, such as stratified sampling and Latin Hypercube Sampling (LHS). In stratified sampling, the range of possible

values for an output can be divided into n sub-intervals, each of which is then sampled a predetermined number of times; this ensures that each sub-interval is represented in the sample for that input, while in LHS each interval of each simulation is sampled only once (NCRP, 2009).

Internal dosimetry typically involves solving a series of ordinary differential equations derived from the compartmental structure of the biokinetic model to obtain the activity in the different model compartments, followed by dose calculations using the conventional ICRP dosimetric approach (ICRP, 2015). Parameter uncertainty analysis can also be performed on the calculated doses using Monte Carlo methods, where the values of the input parameters for the model of interest are first assigned probability distributions. These assigned probability distributions can also take into account correlations between parameters (Puncher and Harrison, 2012a). The model is then solved and doses calculated through multiple iterations using sampled parameters from the assigned probability distributions as opposed to ICRP reference values (Puncher et al., 2008; NCRP, 2009). The resulting output from this approach is a dose distribution that can be characterised using a statistical summary.

However, the dosimetrist should be cautious as the reliability of such analyses depends on the quality of the available data and the judgement of the analyst (Puncher and Harrison, 2012a). Second, care must be taken to ensure that the number of simulations is large enough to ensure convergence of the solution, especially if the Monte Carlo is performed with random sampling, and that reliable software is used for sampling. In addition, correlations between model parameters should be adequately taken into account. Finally, aleatory uncertainty should be distinguished from epistemic uncertainty. The Monte Carlo approach is illustrated in Fig. 1.

6.2. Bayes' theorem

Bayes' theorem is a mathematical rule that explains how one should change existing beliefs in the light of new evidence. It can be used to provide a framework for scientists to combine new data with their existing knowledge or expertise (NCRP, 2009). It is based on probability theory and serves as a common language for expressing uncertainties in model parameters, model structure, or quantities of interest, such as those related to dose or activity. In the Bayesian approach, initial (prior) distributions are first assigned to model parameters, competing model structures and/or intake values. The prior distributions are then updated to incorporate information from measured data. These updated probability distributions are called posterior distributions (Puncher et al., 2013).

It should be noted that in Bayes' theorem the posterior distributions, e.g., biokinetic model parameter values, are proportional to the prior distributions assigned to the parameter values multiplied by the probability distributions for the measurements given the parameter values, which is called the likelihood function (NCRP, 2009). Miller et al. (2001) stated that the advantage of Bayesian methods is that they provide a direct visualization of the relationship between uncertainties in model input parameters and model predictions. However, their disadvantage is that they require a higher level of expertise and computer code than is commonly used.

Birchall et al. (2016) showed that the calculation of the posterior distribution can be numerically difficult, although there are conventional methods for dealing with this type of problem, such as Markov Chain Monte Carlo (MCMC) and Weighted Likelihood Monte Carlo Sampling (WeLMoS). According to Birchall et al. (2016), the application of MCMC is extremely computationally intensive and time consuming for a large cohort. Fortunately, these limitations are now being addressed by the WeLMoS method, which is ideally suited to cases where the uncertainties in the posterior parameter values are relatively large.

The WeLMoS method is particularly suited to situations where there is only a single intake regime. However, the work history of some subjects may consist of several separate and independent unknown intakes, making its application to these situations difficult to implement due to

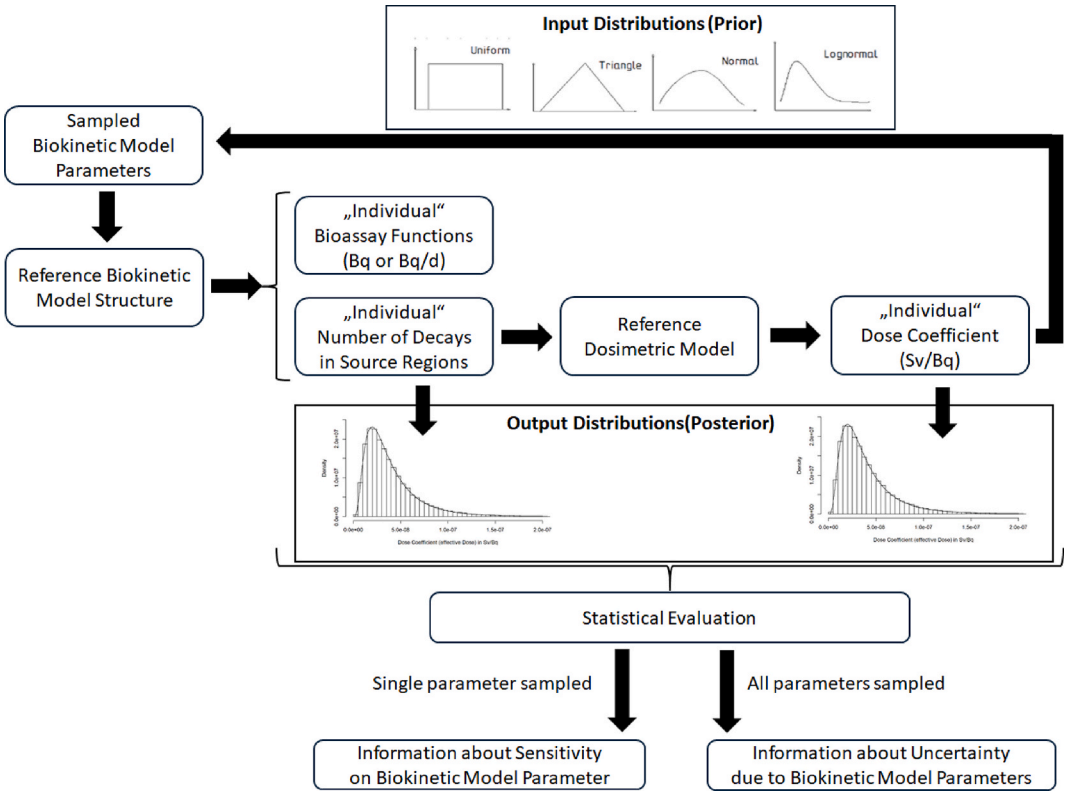

Fig. 1. Monte Carlo simulation technique in internal dosimetry.

the multidimensionality of the probability distribution for intake, and if it were to be extended without modification, there is a likelihood that the method will suffer from convergence problems. The occurrence of such a situation would then require the approximation of multiple intakes into a single intake regime, known as the complex intake regime (CIR) (Puncher et al., 2012; Birchall et al., 2016).

Another drawback of Bayes' theorem is the lack of guidance on the choice of prior distribution (Miller et al., 2001). Although the process of assigning prior probability distribution functions to model parameters can be based on data analysis, i.e., fitting probability distribution curves through existing data, it must rely on a subjective judgement of the state of knowledge that may relate to specific model parameters (Miller et al., 2001; NCRP, 2009). Miller et al. (2001) argue that the prior probability distribution will have little effect on the inferred result when a large amount of measurement data is available.

6.3. Assignment of probability distributions to model parameters

The main challenge for the dosimetrist in performing a parameter uncertainty analysis is to assign appropriate probability distributions to the model parameters of interest. Often dosimetrists use simple common sense rules to assign probability distributions based on judgement, e.g. a uniform probability distribution is used when a parameter is known to vary between a minimum and maximum value but values within this range are considered equally likely (Birchall and James, 1994), while a triangular distribution may be used when parameter values near the middle of the range of possible values are considered more likely than values near either extreme (Morgan and Henrion, 1990). If minimum and maximum values cannot be defined, unbounded distributions, e.g., normal and lognormal, are appropriate, while bounded or truncated distributions must be used if the parameter has physical limits, e.g., a parameter representing a fraction is always greater than zero and less than one. If a parameter value is expected to vary by more than an order of magnitude, it is often best to use a distribution that is most naturally defined on a logarithmic scale, e.g., log-uniform, log-triangular and lognormal (NCRP, 2009).

According to NCRP (2009), the subjectively derived prior distributions may reflect the opinions of a single expert or alternatively a panel of experts. The selection of a probability function based on judgement often describes the degree of belief that possible values of the parameter are within a certain range rather than describing the statistical frequency of measured values.

6.4. Computer codes

Uncertainty and sensitivity analyses have been carried out using several computer programs developed by different authors to implement the Monte Carlo simulation technique on the HRTM parameters in order to obtain the desired distributions. The authors of this review use INTDOSKIT, an R code developed using the RStudio integrated development environment (IDE) to take advantage of the statistical capabilities of the R language (Breustedt et al., 2024). Table 2 provides a summary of codes used to perform uncertainty and sensitivity analyses on doses for selected studies.

7. Parameters affecting calculated equivalent lung dose per unit exposure to radon progeny in underground mines and their probability distributions

Specific parameter values can be introduced in the HRTM in order to provide more realistic doses than those obtained using the ICRP reference values (Bolch et al., 2001, 2003; Fritsch, 2006; Marsh and Birchall, 2009). Uncertainties of the values can be grouped into the following categories;

(i) Uncertainties in the HRTM parameters for the particle deposition model
(ii) Uncertainties in HRTM parameters for the particle transport model
(iii) Uncertainties in the HRTM parameters for the particle dissolution/absorption model
(iv) Uncertainties in HRTM parameters for the dosimetry model

7.1. Uncertainties in the HRTM parameters for the particle deposition model

Skubacz and Wołoszczuk (2019) showed that the dose to the respiratory tract from radon progeny is strongly influenced by the aerosol size distribution, the breathing mode and the breathing rate. As the dose is strongly dependent on the breathing mode, it is usually higher for mouth breathing than for nose breathing at the same breathing rate. Uncertainties in the parameters for the particle deposition model can be grouped into uncertainties in the aerosol parameters, uncertainties in the fraction of air inhaled through the nose, uncertainties in the aerosol deposition efficiencies in different HRTM regions and uncertainties in the anatomical and physiological parameters of the subjects.

7.1.1. Uncertainties in aerosol parameters

The characterization of aerosol parameters for mines is difficult due to highly variable conditions in the mine, different mining methods using diesel or electric powered equipment, different ventilation rates and the type of heating used during the winter months (ICRP, 2017). The radon progeny aerosols are formed in two steps, i.e., after the decay of the radon gas, the freshly formed radionuclides react rapidly (less than 1 s) with trace gases and vapors and grow by cluster formation to form particles of about 1 nm; these are referred to as unattached particles. The unattached particles can also attach to existing aerosol particles in the atmosphere within 1–100 s to form the attached particles (Marsh et al., 2008, Marsh et al.,2012). The process is summarized in Fig. 2.

Marsh et al. (2012) reported that the activity size distribution of attached particles in a mine can be described by a lognormal distribution with an AMAD between 100 and 400 nm. In addition, Butterweck et al. (1992), suggest that the activity size distribution of the attached particles in a mine can be described by a lognormal distribution with an AMAD between 130 and 350 nm, while Skubacz and Wołoszczuk (2019), reported a size range of the attached progeny particles between 50 and 500 nm. Postendörfer et al. (2000), performed experimental studies and observed negligible differences between the activity size distributions of the individual progeny attached to aerosol particles. Postendörfer et al. (2020) then concluded that for simplicity and for dosimetric purposes, the aerosol distribution of each radon progeny is assumed to be the same.

For the unattached aerosols, Marsh et al. (2008) suggests an activity size distribution with an AMTD of 0.8 nm and GSD of 1.3 for all mine conditions, while Skubacz and Wołoszczuk (2019) recommend a size range of 0.5–5 nm. For the purpose of dose calculation and simplicity, the ICRP adopted a unimodal distribution with an AMTD of 1.0 nm and GSD of 1.3 with unit density and unit shape factor for all exposure scenarios for the unattached radon progeny (ICRP, 2017).

The assignment of probability distributions for the aerosol parameters was mainly taken from the work of Marsh (2022), who compiled and analyzed measured data in mines from studies by different authors (Butterweck et al., 1992; Birchall and James 1994; Postendörfer and Reineking 1999). Aerosol parameter values are presented for the two exposure scenarios defined by the epidemiologists in the RADONORM project,[1] i.e., wet drilling with good ventilation and dry drilling with poor ventilation (Deffner, personal communication). These scenarios

[1] www.radonorm.eu.

Table 2
Computer codes for uncertainty and sensitivity analysis in internal dosimetry.

Software	IDE (programming language)	HRTM parameters of interest	Study	Publication
Lung Dose Uncertainty Code (LUDUC)	Microsoft Visual Basic 6 (Fortran 95)	Deposition	Parameter uncertainty analysis	Bolch et al. (2001);
Lung Dose Uncertainty Code (LUDUC)	Microsoft Visual Basic 6 (Fortran 95)	Deposition, particle transport and absorption	Parameter uncertainty analysis	Bolch et al. (2003);
Lung Dose Uncertainty Code (LUDUC)	Microsoft Visual Basic 6 (Fortran 95)	Dosimetry	Parameter uncertainty analysis	Farfan et al. (2003);
Lung Dose Uncertainty Code (LUDUC)	Microsoft Visual Basic 6 (Fortran 95)	Deposition, particle transport, absorption and dosimetry	Parameter sensitivity analysis	Huston et al. (2003)
	Borland Builder 6 (C++)	Deposition	Parameter uncertainty analysis	Fritsch (2006)
Radon Dose Evaluation Program (RADEP)		Deposition, particle transport, absorption and dosimetry	Parameter sensitivity analysis	Marsh and Birchall (2000)
Radon Dose Evaluation Program (RADEP)		Deposition, particle transport, absorption and dosimetry	Parameter uncertainty analysis	Marsh and Birchall (2009)
Integrated Modules for Bioassay Analysis (IMBA)	Microsoft Visual Basic 6	Deposition and Particle transport	Parameter uncertainty and sensitivity analysis	Puncher and Burt (2013)
R-Code (INTDOSKIT)	R Studio(R)	Deposition, Particle Transport, Absorption and dosimetry	Parameter uncertainty and sensitivity analysis	Breustedt et al. (2024)

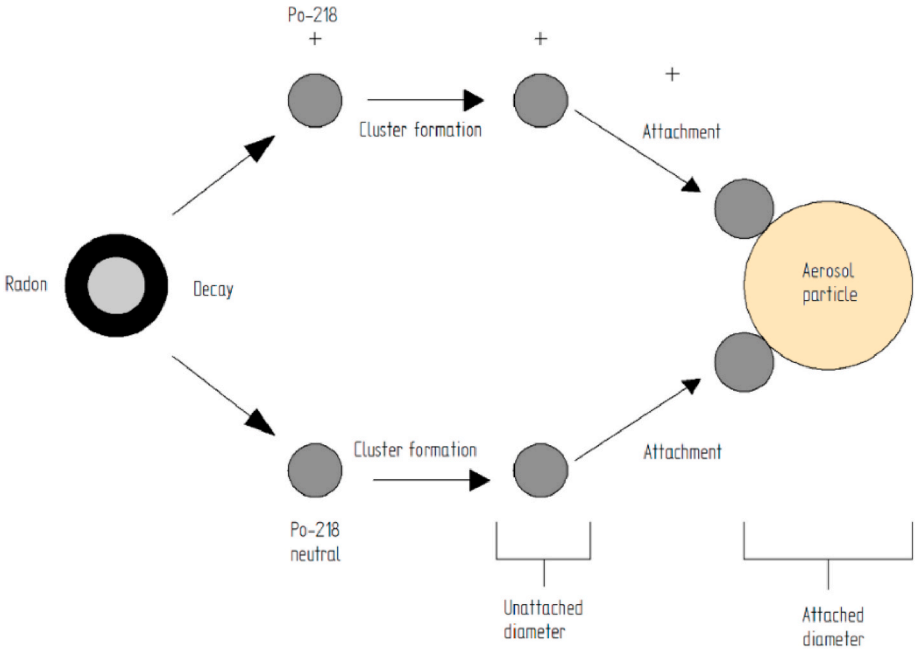

Fig. 2. Basic processes of short-lived radon progeny generation in the air defining the unattached and attached fractions (Skubacz and Wołoszczuk, 2019)

and the according distributions have been adopted by the authors of this paper for their ongoing work.

7.1.1.1. Exposure conditions: wet drilling with good ventilation. Table 3 shows the parameter probability distributions for aerosols that are appropriate for a mine with wet drilling and good ventilation. For this scenario, the size of the unattached fraction depends primarily on the ambient aerosol particle concentration, which is typically low for a mine because the number of particle concentrations is high, i.e., less than 3% of the PAEC (Marsh et al., 2012). The relative size distribution of the unattached radon progeny cluster depends on the concentration of water vapor, trace gases and the electric charge distribution of the radionuclides in the ambient air (ICRP, 2017). Postendörfer (2001) observed that under normal conditions of humidity and radon concentration, the activity size distribution of unattached radon progeny in a mine can be approximated by three lognormal distributions. This observation was based on measured AMTD values of 0.6 nm, 0.85 nm and 1.3 nm and a GSD of 1.2. However, the fraction with an AMTD value of 1.3 nm was never recorded in areas of high radon concentration/humidity.

Although the size of the unattached radon progeny in the lung is assumed to remain constant, some ambient aerosols are hygroscopic and are assumed to grow instantaneously by a given factor upon inhalation (Marsh and Birchall, 2009). As the relative humidity in a mine is high and mine aerosol is likely to be less hygroscopic, Marsh et al. (2008) assumed a hygroscopic growth factor (hgf) of 1.5 for a typical mine. For modelling purposes, d_{th} is assumed to increase instantaneously by the hgf as the particle enters the respiratory tract; as a result, the density will also change (Marsh et al., 2012).

7.1.1.2. Exposure conditions: dry drilling with poor ventilation. Postendörfer reconstructed the working conditions in the former WISMUT uranium mines for dry drilling prior to 1955. Therefore, the central values of the activity size distribution for dry drilling are based on his work (Marsh et al., 2008). The attached mode was reported to be very broad with an AMAD of 560 nm and a GSD of 4.0. This led to the conclusion that the attached progeny for dry drilling consists mainly of silica, which is hydrophobic (Marsh et al., 2008, Marsh et al., 2012). Table 4 shows the parameter probability distributions for aerosols considered appropriate for a dry drilling mine with poor ventilation.

Table 3
Aerosol parameter probability distributions for a mine with wet drilling and good ventilation.

Parameter description	Central value	Probability distribution		
		Form	A[e]	B[f]
Unattached fraction[a], f_p	0.03[c]	uniform	0.005	0.07
Unattached aerosol size, AMTD (nm)	1.0[d]	lognormal	1	1.3
Unattached hygroscopic growth factor, hgf	1.0[c]	constant		
Unattached particle density, ρ (g/cm^3)	1.0[d]	constant		
Unattached shape factor, χ	1.0[d]	constant		
Attached fraction, (1-f_p)	0.97[c]			
Attached aerosol size, AMAD (nm)	350[b]	uniform	235	460
Attached dispersion	2.0[b]	uniform	1.8	3.0
Attached hygroscopic growth factor, hgf	1.5[b]	uniform	1.0	2.0
Attached particle density, ρ(g/cm^3)	1.4[c]	constant		
Attached shape factor, χ	1.1[c]	constant		
Equilibrium factor (F)	0.2[b]	uniform	0.1	0.5

[a] Expressed as a fraction of total PAEC of the radon progeny mixture.
[b] Data taken from Marsh (2022).
[c] Data taken from Marsh et al. (2012).
[d] Data taken from ICRP, 2017.
[e] Minimum value of uniform distribution/geometric mean of lognormal distribution.
[f] Maximum value of uniform distribution/geometric standard deviation for lognormal distribution.

Table 4
Aerosol parameter probability distributions for a mine with dry drilling and poor ventilation.

Parameter description	Central value	Probability distribution		
		Form	A[d]	B[e]
Unattached fraction[a], f_p	0.01[g]	uniform	0.005	0.02
Unattached aerosol size, AMTD (nm)	1.0[b]	lognormal	1	1.3
Unattached hygroscopic growth factor, hgf	1.0[c]	constant		
Unattached particle density, ρ (g/cm^3)	1.0[b]	constant		
Unattached shape factor, χ	1.0[b]	constant		
Attached fraction, (1-f_p)	0.99[c]			
Attached aerosol size, AMAD (nm)	560[c]	lognormal	560	4.0
Attached hygroscopic growth factor, hgf	1.0[c]	constant		
Attached particle density, ρ(g/cm^3)	2.5[c]	constant		
Attached shape factor, χ	1.5[c]	constant		
Equilibrium factor (F)	0.6[g]	uniform	0.4	0.8

[a] Expressed as a fraction of total PAEC of the radon progeny mixture.
[b] Data taken from ICRP, 2017.
[c] Data taken from Marsh et al. (2012).
[d] Minimum value of uniform distribution/geometric standard deviation for lognormal distribution.
[e] Maximum value of uniform distribution/geometric standard deviation for lognormal distribution.
[g] Data taken from Marsh (2022).

7.1.2. Uncertainties in the fraction of air breathed through the nose (F_n)

The nose is considered to be a better filter than the mouth. Therefore, the dose to the lungs is sensitive to the fraction of the ventilatory airflow that passes through the nose (Marsh and Birchall, 2009). The breathing patterns of 30 healthy young adults were studied, 20 of whom were normal augmenters and switched to oro-nasal breathing at a ventilation rate of 2.1 m^3/h during the transition from light to heavy exercise. 5 subjects were pure nose breathers and continued to breathe through the nose even during vigorous exercise, 4 subjects were habitual mouth breathers who breathed oro-nasally at all levels of exercise, while the remaining subject showed no consistent pattern (Niinimaa et al., 1980; 1981).

Ruzer et al. (1995) reported that, on average, a driller spends about 10%, 80% and 10% of his time resting, performing light exercise and heavy exercise respectively. Marsh and Birchall (2009) combined the above information and assigned this parameter a triangular probability distribution with a minimum value of 0.3 and an apex at 1.

7.1.3. Uncertainties in subject anatomical and physiological parameters

The anatomical and physiological characteristics of the subjects that introduce uncertainties in the HRTM deposition model have been presented elsewhere (ICRP, 1994; Bolch et al., 2001; Fritsch, 2006). According to Fritsch (2006), the main anatomical and physiological parameters required by the deposition model are tracheobronchial tree diameters (d_x), dead space volumes for the ET region (VD_ET), BB (VD_BB), bb (VD_bb), total dead space (VD), tidal volume (V_T), ventilation rate (B), volumetric flow rate (V_f) and functional residual capacity (FRC). These parameters can be calculated as a function of the subject's age and height (Bolch et al., 2001; Fritsch, 2006).

Bolch et al. (2001) calculated VD, VD_ET, VD_BB, VD_bb and tracheal diameter (d_0) as functions of subject height (H_t), while Fritsch (2006) calculated BB (d_9) and bb (d_{16}) diameters as functions of d_0; he assigned normal probability distributions to these diameters with standard deviations of 0.1, 0.1 and 0.2 for d_0, d_9 and d_{16} respectively. In their studies, these authors used the calculated values of d_0, d_9 and d_{16} to derive corresponding scaling factors for the subject's airway dimensions with respect to the reference man's dimensions when calculating the aerodynamic and thermodynamic deposition efficiencies.

Ventilation rates can be calculated taking into account the amount of oxygen required according to basal metabolic rate and activity level (Layton, 1993; Bolch et al., 2001; Fritsch, 2006; Marsh and Birchall, 2009). ICRP (1994) considers a standard worker to be one who only breathes through their nose, sits for one third of their daily working time and does light exercise for the remainder of their working time. ICRP (1994) also considers habitual mouth breathers, whose nasal breathing fraction is 0.7 and 0.4 for sitting and light activity respectively. This information was used by Fritsch (2006) to assign uniform probability distributions to these default activity level values. The parameter probability distributions assigned to the subject's anatomical and physiological parameters are shown in Table 5.

7.1.4. Uncertainties in the aerosol deposition efficiencies of different HRTM regions

ICRP (1994) provides various mathematical expressions to calculate both aerodynamic and thermodynamic filtration efficiencies for the different HRTM regions. The aerodynamic and thermodynamic filtration efficiencies are calculated for the different HRTM regions according to equations (3)–(8);

$$\eta_{ae} = 0.5\left[1 - {}^{1}/_{(aR^p + 1)}\right] \tag{3}$$

$$\eta_{th} = 0.5[1 - \exp(-aR^p)] \tag{4}$$

$$\eta_{ae} = 1 - {}^{1}/_{(aR_{th}^p + 1)} \tag{5}$$

$$\eta_{th} = 1 - \exp(-\alpha R^p) \tag{6}$$

$$\eta_{ae} = 1 - \exp(-aR^p) \tag{7}$$

$$\eta_{th} = 1 - \exp(-aR^p) \tag{8}$$

where a and p are constants and R varies with aerosol size and subject characteristics. Equations (3) and (4) apply to particle deposition in ET_1, equations (5) and (6) to particle deposition in ET_2, and equations (7) and

Table 5
Probability distributions on subject parameters of the HRTM deposition model.

Parameter description and calculation	Distribution type	A[e]	B[f]
Age (A, years)	Constant	30	
Body height (H_t, cm)	Normal[b]	176.70	6.70
Body mass index (BMI, kg/m^2)	Lognormal[b]	24.89	1.17
$W_t = H_t^2.BMI$			
Fraction breathed through nose (F_n)	Triangular[c]	0.30	1.00[d]
Airway diameter (cm)			
Trachea: $d_o = (0.00902.H_t + 0.06225).Ed_o$			
Ed_o relative error	Normal[a]	1.00	0.10
Bronchi: $d_9 = (0.00049.H_t + 0.07930).Ed_9$			
Ed_9 relative error	Normal[a]	1.00	0.10
Bronchioles: $d_{16} = (0.0002.H_t + 0.04917).Ed_{16}$			
Ed_{16} relative error	Normal[a]	1.00	0.20
Anatomical dead spaces (ml):			
$V_D = 8.72\exp(0.0162H_t).E_{VD}$			
E_{VD} relative error	Lognormal[b]	1.00	1.17
$V_D(ET) = 18.37.d_o^2$			
$V_D(BB) = V_D(bb) = 0.5[V_D - V_D(ET)]$			
Functional residual capacity (ml):			
$FRC = 23.48H_t + 9.0A - 1093 + E_{FRC}$			
E_{FRC} residual error	Normal[b]	0.00	600.00
Vital Capacity (ml)			
$VC = 61.0H_t - 28.0A - 4650 + E_{VC}$			
E_{VC} residual error term	Normal[b]	0.00[b]	560.00
Ventilation rate (ml/min):			
$V_E = V_Q.V_{O2}$			
$V_{O2} = (0.694.BMR.H_{oxy}).B_{mult}$			
Ventilatory equivalent ratio	Lognormal[b]	26.40	1.16
VQ distribution			
Basal metabolic rate (MJ/d):			
$BMR = 0.063W_t + 2.896 + E_{BMR}$			
E_{BMR} residual error on BMR	Normal[b]	0.00	0.6702
Amount of O_2 required to produce 1 kJ (L)	Uniform[b]	0.0476	0.0529
H_{oxy}			
Basal multiplication factor (B_{mult}):			
Resting	Uniform[b]	1.00	1.10
Sitting	Uniform[b]	1.10	1.40
Light exercise	Uniform[b]	2.00	5.00
Heavy exercise	Uniform[b]	5.50	8.50
Breathing frequency (min^{-1})			
Sitting $B_f = 12E_{Bf}$			
Light exercise $B_f = 20E_{Bf}$			
Heavy exercise $B_f = 26E_{Bf}$			
E_{Bf} relative error	Lognormal[a]	1.00	1.25
Standard worker			
Fraction of sitting during 8 h (remaining light exercise)	Uniform[a]	0.21	0.41
Nose breather			
Sitting fraction breathed through the nose	Uniform[a]	0.90	1.00
Light exercise: Fraction breathed through the nose	Uniform[a]	0.90	1.00
Mouth augmenter			
Sitting fraction breathed through the nose	Uniform[a]	0.60	0.80
Light exercise: fraction breathed through the nose	Uniform[a]	0.30	0.50
Heavy worker			
Fraction of light exercise during 8 h (remaining heavy exercise)	Uniform[a]	0.78	0.98
Nose breather			
Light exercise: fraction breathed through the nose	Uniform[a]	0.90	1.00
Heavy exercise: fraction breathed through the nose	Uniform[a]	0.30	0.50
Mouth augmenter			
Light exercise: fraction breathed through the nose	Uniform[a]	0.20	0.40
Heavy exercise: fraction breathed through the nose	Uniform[a]	0.20	0.40

[a] Data obtained from Fritsch (2006).
[b] Data obtained from Bolch et al. (2001).
[c] Data obtained from Marsh and Birchall (2009).
[d] Parameter assigned a triangular distribution with the vertex representing both the maximum value and mode of the distribution.
[e] Minimum value for a uniform/triangular distribution or mean for the normal distribution or geometric mean for the lognormal distribution.
[f] Maximum value for a uniform/triangular distribution or standard deviation for the normal distribution or geometric standard deviation for the lognormal distribution.

(8) to particle deposition in the thoracic region. In each region of the HRTM, the total deposition is a combination of the two independent equations.

Fritsch (2006) showed that the uncertainties in these values are handled by multiplying the fitting parameters a_i in Tables 12 and 13 of ICRP Publication 66 (ICRP, 1994) by the random variables $C_{ae}(j)$ and $C_{th}(j)$ for aerodynamic and thermodynamic deposition mechanisms, respectively, in each HRTM region, which are assigned lognormal distributions with a mean of one and a GSD given by the square root of c_j (Table 14 of ICRP Publication 66). These distributions are summarized in Table 6.

7.2. Uncertainties in HRTM particle transport parameters

ICRP has derived the particle transport rates in the HRTM from a number of studies using laboratory animals and, to some extent, an element of expert judgement (Bolch et al., 2003; Puncher and Burt, 2013). The key assumption made by the ICRP in their derivation is that the variability in particle transport within the HRTM varies by a factor of 3 around the reference value, so the uncertainty in these rates can be represented by a lognormal distribution with a median given by the ICRP reference value and a GSD of 1.73 (Puncher and Burt, 2013).

However, Puncher and Burt (2013) stated that the movement of material from the AI region to the bb region and thoracic lymph nodes (LN_{TH}) occurs by different processes to those governing particle transport from the bb and BB airways, with the former being facilitated by microphages in the AI region and the latter by mucociliary transport along the airway walls. On this basis, Puncher (2014a) suggested that the variability in the rate of clearance from the alveolar (ALV) to bb region can be assigned a lognormal distribution with a median equal to the ICRP reference value and a GSD of 4.5, while the rate from the ALV to the interstitium (INT) can be represented by a lognormal distribution with a median equal to the ICRP reference value and a GSD of 3.2. Because of the slow rate, the variability in the rate from INT to LN_{TH} was represented by a lognormal distribution with a median equal to the ICRP reference value and a GSD of 3.0.

The particle transport rates relevant to the uncertainties in the calculated lung dose for radon progeny inhalation are the rate from BB to ET_2 and the rate from ET_2 to the alimentary tract, the other rates being considered too slow to significantly alter the calculated lung dose, since it is assumed that the deposited material decays in situ. The probability distributions associated with these rates are shown in Table 7.

Table 6
Probability distributions of the aerosol deposition efficiencies in the different HRTM regions.

Parameter	Distribution	Median	GSD
$C_{ae}(ET_1)$	Lognormal	1.00	1.82
$C_{ae}(ET_2)$	Lognormal	1.00	1.82
$C_{ae}(BB)$	Lognormal	1.00	1.58
$C_{ae}(bb)$	Lognormal	1.00	1.58
$C_{ae}(AI)$	Lognormal	1.00	1.30
$C_{th}(ET_1)$	Lognormal	1.00	1.18
$C_{th}(ET_2)$	Lognormal	1.00	1.18
$C_{th}(BB)$	Lognormal	1.00	1.23
$C_{th}(bb)$	Lognormal	1.00	1.23
$C_{th}(AI)$	Lognormal	1.00	1.23

Table 7
Probability distributions on particle transport rates of the HRTM.

From	To	Reference value[a] (d^{-1})	Distribution	Median	GSD
bb	BB	0.2	Lognormal[b]	1.00	1.73
BB	ET_2	10	Lognormal[b]	1.00	1.73
ET_2	Oesophagus	100	Lognormal[b]	1.00	1.73
ET_1	ET_2	1.5	Lognormal[b]	1.00	1.73
ET_1	Environment	0.6	Lognormal[b]	1.00	1.73
BBseq	LN_{TH}	0.001	Lognormal[b]	1.00	1.73
bb_{seq}	LN_{TH}	0.001	Lognormal[b]	1.00	1.73
ETseq	LNET	0.001	Lognormal[b]	1.00	1.73
ALV	bb	0.002	Lognormal[c]	0.002	4.50
ALV	INT	0.001	Lognormal[c]	0.001	3.20
INT	LN_{TH}	0.00003	Lognormal[c]	0.00003	3.00

[a] The reference value was obtained from ICRP publication 130 (ICRP, 2015).
[b] The uncertainty on these correlated parameters was introduced by multiplying the ICRP reference value with a value obtained from a random variable sampled from a lognormal probability distribution with a median of 1.0 and GSD of 1.73.
[c] Data taken from Puncher (2014a).

7.3. Uncertainties in target cell parameters

It is assumed that both the depth and thickness of the target cell layer are correlated with the epithelial thickness; the epithelial thickness is used here to introduce a correlation between the depth of the target cell layer and the thickness of the target cell layer (Marsh and Birchall, 2009). ICRP (1994) adopted a reference value of 55 μm for the epithelial thickness of the BB region of the HRTM using data from Mercer et al. (1991), although a lower value for this parameter was reported in the measurements of Harley et al. (1996).

Harley et al. (1996) also reported a mean basal cell depth of 27 μm in the region of airway generations 3 to 6, whereas the HRTM assumes that the basal cells are uniformly distributed in a 15 μm layer at a depth of 35 μm (i.e., mean depth of 43 μm) in the BB region, which is consistent with the data of Mercer et al. (1991).

Marsh and Birchall (2009) used this information and assumed a rectangular distribution for bronchial epithelial thickness with values ranging from 30 to 75 μm, the idea being to reflect both intra- and inter-subject variability, with the lower value being consistent with the data of Harley et al. (1996). The distribution assumed for the epithelial thickness of the BB region was also based on the data of Mercer et al. (1991) and reflects intra- and inter-subject variation, while the judgement made in assigning the probability distribution for the thickness of the mucus sol was based on measurements reported in ICRP Publication 66 (ICRP, 1994). The probability distributions assumed for these parameters are given in Table 8.

7.4. Uncertainties in absorption parameters for radon progeny

The HRTM dissolution/absorption parameters relevant to dose calculation are;

i) Dissolution parameters, i.e., the fraction of rapidly dissolving material, f_r, the dissolution rate of the rapid fraction, s_r, and the dissolution rate of the slow fraction, s_s.
ii) Bound state parameters such as the fraction of bound material, f_b, and the absorption rate of bound material into blood, s_b.

Studies have been carried out to determine the absorption parameters from the lung for both unattached and attached radon progeny after inhalation and the results have been published in literature (Butterweck et al., 2002; Marsh and Bailey, 2013). Marsh and Birchall (2009) published the probability distributions for the dissolution and absorption parameters for radon progeny; these distributions are given in Table 9.

An important question is whether a fraction of the attached radon progeny is bound to the airways of the respiratory tract, and whether the attached radon progeny deposited in the respiratory tract will separate from the aerosol and subsequently adopt the same absorption characteristics as the unattached progeny. Marsh and Bailey (2013) argue that rapid detachment could occur due to alpha recoil and/or physicochemical interactions of the material with the lung fluid. These concerns have been addressed by the ICRP in its Publication 137 (ICRP, 2017).

ICRP (2017) also assigns independent parameters to polonium, lead

Table 8
Probability distributions of the HRTM target cell parameters.

Description of parameter	HRTM reference value (μm)	Probability distribution		
		Form	A[d]	B[e]
Bronchial epithelium thickness (E_{BB})[a]	55	uniform	30 μm	75 μm
Bronchial basal cell layer depth[b]	35	$35E_{BB}/55$		
Bronchial basal cell layer thickness	15	$15E_{BB}/55$		
Bronchial secretory cell layer depth[c]	10	$10E_{BB}/55$		
Bronchial secretory cell layer thickness	30	$30E_{BB}/55$		
Bronchial mucus (gel) thickness	5	Lognormal	4 μm	2
Bronchial mucus (sol) thickness	6	Normal	6 μm	1 μm
Bronchiolar epithelium thickness (E_{bb})[a]	15	Uniform	8 μm	22 μm
Bronchiolar secretory cell layer depth[c]	4	$4E_{bb}/15$		
Bronchiolar secretory cell layer thickness	8	$8E_{bb}/15$		
Bronchiolar mucus (gel) thickness	2	Lognormal	1.6 μm	2
Bronchiolar mucus (sol) thickness	4	Normal	4 μm	1 μm

[a] Parameter not used directly in the model but are used to introduce correlation between model parameters which are functions of them.
[b] Depth of basal cell layer is defined here as in ICRP Publication 66 as the distance from the luminal surface of the epithelium (excluding cilia) to the beginning of the basal cell layer.
[c] Depth of secretory cell layer is defined here as in ICRP Publication 66 as the distance from the luminal surface of the epithelium (excluding cilia) to the beginning of the secretory cell layer.
[d] Minimum value of uniform distribution/mean of normal distribution/geometric mean of lognormal distribution.
[e] Maximum value of uniform distribution/standard deviation of normal distribution/geometric standard deviation of lognormal distribution.

Table 9
Probability distributions for radon progeny dissolution[a]/absorption parameters (Marsh and Birchall, 2009).

Description of parameter	Representative value	Probability distribution		
		Form	A	B
Unattached, f_r	1.00[b]	Constant		
Unattached, $s_r(d^{-1})$	1000[b]	Constant		
Unattached, f_b	0.80[b]	Uniform	0.70	0.85
Unattached, $s_b(d^{-1})$	1.70[b]	Fixed		
Attached, f_r	0.06[c]	Uniform	0.00	0.10
Attached, $s_r(d^{-1})$	67.00[c]	Fixed		
Attached, $s_s(d^{-1})$	1.40[c]	Uniform	1.10	3.30
Attached, f_b	0.00[c]	Constant		

[a] The HRTM defines absorption in terms of the following parameters; f_r = rapid dissolution fraction, s_r = rapid dissolution rate, s_s = slow dissolution rate, f_b = bound fraction; s_b = uptake from bound state.
[b] Unattached progeny parameters are based on the results of volunteer experiments performed by Butterweck et al. (2002).
[c] Attached parameter values are based on the review of published data by Marsh and Bailey (2013).

and bismuth as radon progeny, assuming that lead progeny binds to the respiratory tract. In addition, ICRP assumes common kinetics for radon progeny formed in the HRTM and independent kinetics for absorption from the digestive tract to the blood for material cleared from the HRTM to the digestive tract by mucocilliary transport (ICRP, 2015, 2017). Furthermore, only a fast component is assumed with a biological half-life of 5.5 h for polonium isotopes and 17 h for bismuth isotopes without a bound state. Fast absorption with a biological half-life of 10 min is assumed for 10% of the lead isotopes, the remainder being absorbed with a biological half-life of 9.8 h. For the bound state, retention in the airway walls is assumed to have a biological half-life of 9.8 h (Hu et al., 2020). Table 10 shows the dissolution/absorption parameters for radon progeny published in ICRP Publication 137.

8. Challenges and limitations in current research practices

Some of the challenges encountered in the uncertainty assessment of dose coefficients for radon intake and progeny include the following;

The availability of different algorithms for solving the biokinetic models and hence the Monte Carlo simulations, i.e., several tools are now available that can be used to solve the biokinetic models using different algorithms. However, dosimetrists are faced with the challenge of finding an appropriate compromise between numerical accuracy and computational time. Studies on the comparison of different dose calculation tools have been carried out by Hu et al. (2020), who compared the results of the dose conversion factors (DCF) of IMBA with published values obtained from RADEP and LUDEP for the inhalation of radon and thoron progenies. These authors concluded that IMBA is much faster and more optimal than RADEP and LUDEP.

Another challenge is the choice of probability distributions for radon progeny dissolution/absorption parameters. In their study, Marsh et al. (2002) used the same parameters for bismuth, lead and polonium derived from a half-life of 10 h, assuming no binding of activity to the lung. However, studies conducted later by Marsh and Bailey (2013) provide evidence of binding of lead ions to the lung. Furthermore, other studies have shown that binding can increase the lung dose by up to 30% due to the retained activity being closer to the target cells (Marsh et al., 2002, 2005; Marsh and Birchall, 2009). The latest dissolution/absorption parameters for radon and thoron progeny have also been published by ICRP, but no information has yet been provided on the probability distributions for these parameters.

In addition, the chemical form of the inhaled aerosols presents a further challenge to uncertainty analysis, as it determines the rate of uptake of the radionuclide into blood and hence the lung dose. This is because blood uptake and mechanical transport are competing particle clearance processes in the HRTM (Bolch et al., 2003). Information from many literature sources shows that the chemical form is uncertain for most nuclides, including radon progeny, with the ICRP recommending the use of standard absorption type M solubility parameters in the absence of specific data (ICRP, 2015). Therefore, lack of knowledge of the chemical form of inhaled material is always a major source of uncertainty in dose calculations.

Furthermore, mine aerosol parameters are difficult to characterize (Marsh et al., 2008). This is a challenge because aerosol size determines the amount of radioactive material deposited in different regions of the respiratory tract and hence the lung dose.

A number of epidemiological studies of uranium miners have been conducted to assess the risk of lung cancer from inhalation of radon and its progeny. However, miners also receive radiation doses from the inhalation of long-lived radionuclides in uranium ore dust and from external gamma radiation (Marsh et al., 2012). Marsh et al. (2005) argued that the additional lung dose from these long-lived alpha emitters could be about 10% of that from the short-lived radon progeny. Omission of the doses from these long-lived radionuclides and external gamma radiation could therefore lead to an underestimation of the calculated lung dose.

Finally, Honorio da Silva et al. (2023) in their study compared the lung doses of healthy smokers and non-smokers for radon progeny intake under the same exposure conditions in mines, homes and tourist caves, and their results confirmed that smokers receive 3% less lung dose than the ICRP reference worker in mines. Therefore, the health status and lifestyle of the exposed person may be another source of uncertainty in the calculated doses.

9. Comparative analysis

A parameter uncertainty analysis assumes that the model is a realistic representation of the physical and biological processes and that only the parameter values are uncertain (Marsh et al., 2010). Several model structures have been published for the respiratory tract, resulting in uncertainties due to the model structure. To account for the uncertainty in the model structure, it is useful to compare results from different models with similar parameter values, e.g., Winkler-Heil et al. (2007) compared the results of the effective dose for radon progeny inhalation (mSv/WLM) obtained using the ICRP Publication 66 HRTM, a deterministic airway generation model and a stochastic airway generation model with the same input parameters and obtained similar results ranging from 8.3 to 11.8 mSv/WLM. However, the authors noted that one of the important issues affecting the comparison is the averaging procedure for the calculated doses in the airway generation models.

James et al. (2004) also calculated effective doses from radon progeny for mines and homes using ICRP Publication 66 HRTM. These authors assumed the activity size distribution given in the Biological Effects of Ionizing Radiation (BEIR) IV report and calculated a lung dose of 21 mSv/WLM for mines and homes, which was higher than other estimates. The authors attributed this difference to the assumed activity size distributions. On the other hand, Marsh et al. (2005) used ICRP Publication 66 HRTM and obtained a lower dose value of 13 mSv/WLM for mines and homes using activity size distributions based on measurements made in Europe. The above results show that the uncertainty in the particle size distribution for radon progeny can have a significant influence on the calculated lung dose.

Other authors, such as Honorio da Silva et al. (2023), used the stochastic lung deposition model to compare the lung doses of a healthy smoker and the ICRP reference worker after exposure to radon gas and progeny in a mine. In their study, information on changes in the respiratory tract induced by chronic cigarette smoking was collected from literature and used to calculate the dose received by the lungs and other organs outside the respiratory tract. The morphological and physiological parameters affected by chronic cigarette smoking were implemented in the HRTM, and the authors reported that smokers received 3% lower lung doses than the ICRP reference worker in mines; a similar dose reduction was found for the ET region of the HRTM. These results highlight the importance of inter-subject variability and its contribution

Table 10
HRTM dissolution/absorption parameters for inhaled radon progeny (ICRP, 2017).

Radon progeny	Dissolution parameter values			Uptake parameter values		Absorption from the alimentary tract, f_A
	f_r	$s_r(d^{-1})$	$s_s(d^{-1})$	f_b	$s_b(d^{-1})$	
Polonium	1.00	3.00	0.00	0.00	0.00	0.10
Lead	0.10	100	1.70	0.50	1.70	0.20
Bismuth	1.00	1.00	0.00	0.00	0.00	0.05

to the uncertainty in the calculated lung dose.

10. Regulatory implications

A comprehensive review of the scientific evidence on lung cancer and radon exposure has been published by the ICRP (ICRP, 2010). In this review, the recommended maximum radon concentration, a key figure driving public health policy on indoor radon, was reduced from 600 Bq/m^3 to 300 Bq/m^3. These recommendations were updated in Publication 126 (ICRP, 2014), taking into account the key scientific findings of ICRP (2010) and the latest ICRP principles and methodology. The above recommendations called on authorities to set a national reference level as low as reasonably achievable in the range of 100–300 Bq/m^3. This was because a comparison of radon concentrations in the workplace with reference levels was necessary to control radon in homes and workplaces.

In response to the above recommendations, several pieces of legislation have been enacted by both national and regional authorities to protect workers and members of the public from the effects of ionizing radiation. For example, the European Union (EU) adopted the Council Directive 2013/59/EURATOM as the basic safety standard for protection against the dangers arising from exposure to ionizing radiation.[2] Considering the importance of the uncertainty assessment of the calculated doses, the results of such studies are crucial for the regulatory authorities, as they provide information on the reliability of the assessed doses and point to sensitive parameters for a better fit of the models to the monitoring data. This in turn provides insight into the setting of appropriate dose limits.

11. Conclusion and future outlook

The aim of this work was to identify the parameters that affect the calculated equivalent lung dose per unit exposure to radon progeny in a mine. The lung dose per unit exposure to radon and progeny can be calculated using the methods described in ICRP Publication 130. Literature studies reviewed in this work indicate that at least 98% of the lung dose is attributable to the inhalation of radon and thoron progeny in mines. From the literature, the parameters influencing the calculated lung dose include aerosol parameters, i.e., particle size, unattached fraction, particle density and shape factor; subject parameters, i.e., breathing mode and nasal fraction. Other parameters affecting the lung dose include the absorption rates of radon progeny into the blood, the mechanical transport rates from the BB region to ET_2 and from ET_2 to the alimentary tract, and the depth and thickness of the target cells. Finally, the techniques that can be used to quantify the uncertainties in the calculated lung dose, such as Bayes' theorem and Monte Carlo simulations, are discussed.

It has been suggested in literature that a quantitative analysis of the uncertainties in the model parameters for radon progeny inhalation can help to guide regulators in setting appropriate limits for radon exposure in mines. Secondly, the information on parameter sensitivity can help to guide stakeholders on where research efforts should be focused when updating the models and their associated parameters in order to reduce these uncertainties. In addition, information on both uncertainty and sensitivity of model parameters and outputs can help policy makers and health physicists to design appropriate monitoring programmes for miners. Furthermore, quantification of the uncertainties in the calculated doses resulting from the sources of uncertainty in the model parameters can be used to assess the reliability of dose coefficients used in radiation protection to ensure that miners' radon exposure meets regulatory standards. Therefore, understanding and reducing parameter uncertainties in the dosimetry of radon exposure will be essential for accurate risk assessment and implementation of effective safety measures in underground mines.

The information on the assignment of probability distributions from this review is currently being used by the authors in their ongoing study to quantify the uncertainties in the calculated doses arising from the uncertainties in the biokinetic model parameters for the two exposure scenarios defined in Section 7 for both radon and thoron progeny. The authors noted that the literature reviewed included studies performed using ICRP Publication 66 HRTM. In addition, the studies on uncertainty and sensitivity analysis of the equivalent lung dose per unit exposure to radon progeny in a mine showed that the same value of the dissolution/absorption parameters was assumed for all radon progeny. The authors of this review intend to use the latest parameters given by ICRP in its Publications 130 and 137 in their ongoing study.

As miners are also exposed to radiation from other long-lived radionuclides, the studies carried out by the authors of this review also aim to quantify the uncertainties in organ doses from long-lived radionuclides of the U-238, Th-232 and U-235 decay series. The organs of particular interest in this work are the lung, liver, bone surface, stomach, colon, heart, kidney, brain and lymphatic tissue.

Finally, ongoing research by the authors of this publication will focus on the sources of uncertainty in the exposure scenario and the biokinetics of radon progeny, but not on the uncertainties in the dosimetric model. This is because, to the best of the authors' knowledge, no significant changes have been made to the dosimetric model for radon progeny that would warrant further investigation. Secondly, the uncertainties in the biokinetics and exposure scenarios are more dominant than those arising from the dosimetric model, since the dosimetric model uses nuclear decay data that are known with certainty. In addition, the radiation weighting factors have been published by ICRP without uncertainties. Therefore, the only parameter in the dosimetric model that could be of interest for further investigation is the specific absorbed fraction (SAF). However, in the case of radon progeny, the dose is mainly contributed by the alpha particles, which are completely absorbed in the source regions. Therefore, the authors have found it reasonable to neglect the uncertainties contributed by the dosimetric model, since alpha particles are the main contributors to the calculated doses. The results of this ongoing work will be published in the framework of the ongoing Euratom research program RADONORM.

CRediT authorship contribution statement

Thomas Makumbi: Writing – review & editing, Writing – original draft, Validation, Methodology, Investigation, Formal analysis, Data curation. **Bastian Breustedt:** Writing – review & editing, Supervision, Software, Methodology, Conceptualization. **Wolfgang Raskob:** Writing – review & editing, Supervision, Project administration, Funding acquisition.

Declaration of competing interest

The authors declare that they have no known competing financial interests or personal relationships that could have appeared to influence the work reported in this paper.

Data availability

No data was used for the research described in the article.

Acknowledgements

This work has received funding from the Euratom research and training programme 2019–2020 under grant agreement No 900009 (RADONORM).

[2] https://www.ensreg.eu/nuclear-safety-regulation/eu-instruments/Basic-Safety-Standards-Directive.

References

Abdo, M.A.S., Boukhair, A., Fahad, M., Ouakkas, S., Arhouni, F.E., Hakkar, M., Belhabib, M., Al-Suhbani, M.N., 2021. Estimation of unattached and aerosol-attached activities of airborne short-lived radon progeny in indoor environments. J. Environ. Radioact. 237, 106665 https://doi.org/10.1016/j.jenvrad.2021.106665.

Bailey, M.R., Puncher, M., 2007. Uncertainty analysis of the ICRP human respiratory tract model applied to interpretation of bioassay data for depleted uranium. Health Protection Agency, UK. https://assets.publishing.service.gov.uk/media/5a7e0fade d915d74e33efcd6/HpaRpd023.pdf.

Bersimbaev, R.I., Bulgakova, O., 2015. The health effects of radon and uranium on the population of Kazakhstan. Gene Environ. 37, 18. https://doi.org/10.1186/s41021-015-0019-3.

Bi, L., Li, W.B., Tschiersch, J., Li, J.L., 2010. Age and sex dependent inhalation doses to members of the public from indoor thoron progeny. J. Radiol. Prot. 30, 639–658. https://doi.org/10.1088/0952-4746/30/4/001.

Birchall, A., James, A.C., 1994. Uncertainty analysis of the effective dose per unit exposure from radon progeny and its implication for ICRP risk-weighting factors. Radiat. Protect. Dosim. 53 (1–4), 133–140. https://doi.org/10.1093/rpd/53.1-4.133.

Birchall, A., Puncher, M., Vostrotin, V., 2016. The mayak worker dosimetry system (MWDS-2013): treatment of uncertainty in model parameters. Radiat. Protect. Dosim. 176 (1–2), 144–153. https://doi.org/10.1093/rpd/ncw248.

Bolch, W.E., Farfan, E.B., Huh, C., Huston, T.E., Bolch, W.E., 2001. Influences of parameter uncertainties within the ICRP 66 respiratory tract model: particle deposition. Health Phys. 81 (4), 378–394. https://doi.org/10.1097/00004032-200110000-00003.

Bolch, W.E., Huston, T.E., Farfan, E.B., Vernetson, W.G., Bolch, W.E., 2003. Influences of parameter uncertainties within the ICRP-66 respiratory tract model: particle clearance. Health Phys. 84 (4), 421–435. https://doi.org/10.1097/00004032-200304000-00002.

Breustedt, B., Blanchardon, E., Castellani, C.M., Etherington, G., Franck, D., Giussani, A., Hofmann, W., Lebacq, A.L., Li, W.B., Noßke, D., Lopez, M.A., 2017. EURADOS work on internal dosimetry. Ann. ICRP 47 (3–4), 75–82. https://doi.org/10.1177/0146645318756232.

Breustedt, B., Chavan, N., Makumbi, T., 2024. An R Code for calculation of dose coefficients and studying their uncertainties. Health Phys. Manuscr. Accept. Publ.

Breustedt, B., Giussani, A., Noßke, D., 2018. Internal dose assessment - concepts, models and uncertainties. Radiat. Meas. 115, 49–54, 101016/jradmeas201806013.

Brudecki, K., Li, W.B., Meisenberg, O., Tschiersch, C., Hoeschen, C., Oeh, U., 2014. Age-dependent inhalation doses to members of the public from indoor short-lived radon progeny. Radiat. Environ. Biophys. 53, 535–549. https://doi.org/10.1007/s00411-014-0543-8.

Butterweck, G., Porstendörfer, J., Reineking, A., Kesten, J., 1992. Unattached fraction and the aerosol size distribution of the radon progeny in a natural cave and mine atmospheres. Radiat. Protect. Dosim. 45 (1–4), 167–170. https://doi.org/10.1093/rpd/45.1-4.167.

Butterweck, G., Schuler, Ch, Vezzu, G., Müller, R., Marsh, J.W., Thrift, S., Birchall, A., 2002. Experimental determination of the absorption rate of unattached radon progeny from respiratory tract to blood. Radiat. Protect. Dosim. 102 (4), 343–348. https://doi.org/10.1093/oxfordjournals.rpd.a006103.

Carillo, C.A., Inostrosa, M.A., Rangel, Y.B., 2015. Radon and its effects on the health of uranium mine workers. Med. Segur. Trab. 61 (238), 99–111.

Chen, J., 2023. A review of radon exposure in non-uranium mines: estimation of radon exposure in Canadian mines. Health Phys. 124 (4), 244–256. https://doi.org/10.1097/HP.0000000000001661.

Deffner, V., 2022. Personal Conversation.

Everitt, B.S., 1995. The Cambridge Dictionary of Statistics in Medical Sciences. Cambridge University Press, New York. ISBN-13:978-0521479288.

Evrard, A.S., Hemon, D., Billon, S., Laurier, D., Jougla, E., Tirmarche, M., Clavel, J., 2006. Childhood leukemia incidence and exposure to indoor radon, terrestrial and cosmic gamma radiation. Health Phys. 90 (6), 569–579. https://doi.org/10.1097/01.HP.0000198787.93305.35.

Farfan, E.B., Huston, T.E., Bolch, W.E., Vernetson, W.G., Bolch, W.E., 2003. Influences of parameter uncertainties within the ICRP-66 respiratory tract model: regional tissue doses for 239-PuO_2 and 238-UO_2/238-U_3O_8. Health Phys. 84 (4), 436–450. https://doi.org/10.1097/00004032-200304000-00003.

Fritsch, P., 2006. Uncertainties in aerosol deposition within the respiratory tract using the ICRP 66 model: a study in workers. Health Phys. Soc. 114–126. https://doi.org/10.1097/01.hp.0000174810.12283.18.

Harley, N., Cohen, B.S., Robbins, E.S., 1996. The variability in radon decay product bronchial dose. Environ. Int. 22, 959–964. https://doi.org/10.1016/S0160-4120(96)00208-5.

Harrison, J.D., Day, P., 2008. Radiation doses and risks from internal emitters. J. Radiol. Prot. 28, 137–159. https://doi.org/10.1088/0952-4746/28/2/R01.

Harrison, J.D., Marsh, J.W., 2012. Effective dose from inhaled radon and its progeny. Ann. ICRP 41 (3–4), 378–388. https://doi.org/10.1016/j.icrp.2012.06.012.

Harrison, J.D., Leggett, R.W., Noßke, D., Paquet, F., Phipps, A.W., Taylor, D.M., Metivier, R., 2001. Reliability of the ICRP dose coefficients for members of the public, II. Uncertainties in the absorption of ingested radionuclides and the effect on dose estimates. Radiat. Protect. Dosim. 95 (4), 295–308. https://doi.org/10.1093/oxfordjournals.rpd.a006554.

Hofmann, W., Lettner, H., Hubmer, A., 2021. Dosimetric comparison of exposure pathways to human organs and tissues in radon therapy. Int. J. Environ. Res. Publ. Health 18, 10870. https://doi.org/10.3390/ijerph182010870.

Honorio da Silva, E., Davesne, E., Bonchuk, Y., Ratia, G., Madas, B., Berkovskyy, V., Broggio, D., 2023. Changes induced in the human respiratory tract by chronic cigarette smoking can reduce the dose to the lungs from exposure to radon progeny. J. Radiol. Prot. 43, 021509 https://doi.org/10.1088/1361-6498/acd3fa.

Hu, J., Iwaoka, K., Hosoda, M., Tokonami, S., 2020. Lung dose estimation of ^{222}Rn and ^{220}Rn progeny based on IMBA Professional Software. Radiat. Environ. Med. 9 (1), 21–27. https://doi.org/10.51083/radiatenvironmed.9.1_21.

Hu, J., Wu, Y., Saputra, M.A., Song, Y., Yang, G., Tokonami, S., 2022. Radiation exposure due to ^{222}Rn, ^{220}Rn and their progenies in three metropolises in China and Japan with different air quality levels. J. Environ. Radioact. 244–245, 106830 https://doi.org/10.1016/j.jenvrad.2022.106830.

Hussein, A.S., 2008. Radon in the environment: friend or foe?. In: Proceedings of the 3rd Environmental Physics Conference, February 19-23, 2008, Aswan, Egypt Available at: https://inis.iaea.org/collection/NCLCollectionStore/_Public/41/046/41046584.pdf.

Huston, T.E., Farfan, E.B., Bolch, W.E., Bolch, W.E., 2003. Influences of parameter uncertainties within the ICRP-66 respiratory tract model. Health Phys. 85 (5), 553–566. https://doi.org/10.1097/00004032-200311000-00003.

ICRP, 1994. Human respiratory tract model for radiological protection. ICRP Publication 66. Ann. ICRP 24 (1–3).

ICRP, 2010. Lung cancer risk from radon and progeny & statement on radon. ICRP Publication 115. Ann. ICRP 40 (1).

ICRP, 2014. Radiological protection against radon exposure. ICRP Publication 126. Ann. ICRP 43 (3).

ICRP, 2015. Occupational intakes of radionuclides: Part 1. ICRP Publication 130. Ann. ICRP 44 (2).

ICRP, 2017. Occupational intakes of radionuclides: Part 3. ICRP Publication 137. Ann. ICRP 46 (3/4).

James, A.C., Birchall, A., Akabani, G., 2004. Comparative dosimetry of BEIR IV revisited. Radiat. Protect. Dosim. 108 (1), 3–26. https://doi.org/10.1093/rpd/nch007.

Kendall, G.M., Smith, T.J., 2002. Doses to organs and tissues from radon and its decay products. J. Radiol. Prot. 22, 389–406. https://doi.org/10.1088/0952-4746/22/4/304.

Khursheed, A., 2000. Doses to systemic tissues from radon gas. Radiat. Protect. Dosim. 88 (2), 171–181. https://doi.org/10.1093/oxfordjournals.rpd.a033035.

Kleinschmidt, R., Watson, D., Janik, M., Gillmore, G., 2018. The presence and dosimetry of radon and thoron in a historical underground metalliferous mine. J. Sustain. Min. 17, 120–130. https://doi.org/10.46873/2300-3960.1130.

Kwon, T., Chung, Y., Yoo, J., Ha, W., Cho, M., 2020. Uncertainty quantification of bioassay functions for the internal dosimetry of radioiodine. J. Radiat. Res. 61 (6), 860–870. https://doi.org/10.1093/jrr/rraa081.

Layton, 1993. Metabolically consistent breathing rates for use in dose assessments. Health Phys. 64, 23–26. https://doi.org/10.1097/00004032-199301000-00003.

Leggett, R.W., 2001. Reliability of the ICRP's dose coefficients for members of the public: I. Sources of uncertainty in the biokinetic models. Radiat. Protect. Dosim. 95 (3), 199–213. https://doi.org/10.1093/oxfordjournals.rpd.a006543.

Leggett, R.W., 2003. Reliability of the ICRP's dose coefficients for members of the public: III. Plutonium as a case study of uncertainties in the systemic biokinetics of radionuclides. Radiat. Protect. Dosim. 106 (2), 103–120. https://doi.org/10.1093/oxfordjournals.rpd.a006340.

Leggett, R.W., Harrison, J., Phipps, A., 2007. Reliability of the ICRP's dose coefficients for members of the public: IV. Basis of the human alimentary tract model and uncertainties in model predictions. Radiat. Protect. Dosim. 123 (2), 156–170. https://doi.org/10.1093/rpd/ncl104.

Leggett, R.W., Marsh, J.W., Gregoratto, D., Blanchardon, E., 2013. A generic biokinetic model for noble gases with application to radon. J. Radiol. Prot. 33, 413–432. https://doi.org/10.1088/0952-4746/33/2/413.

Li, W.B., 2018. Internal dosimetry: a review of progress. Health Phys. 53 (2), 72–99. https://doi.org/10.5453/jhps.53.72.

Li, W.B., Klein, W., Blanchardon, E., Puncher, M., Leggett, R.W., Oeh, U., Breustedt, B., Noßke, D., Lopez, M.A., 2015. Parameter uncertainty analysis of a biokinetic model of cesium. Radiat. Protect. Dosim. 163 (1), 37–57. https://doi.org/10.1093/rpd/ncu055.

Liu, G., Niu, L.M., Cao, X.B., Liu, Y.Y., Wu, X.Q., Zhang, X., Zhang, R., 2022. Study of the occupational health risk of radon exposure in underground workers in a mine. J. Radiat. Res.Appl. Sci. 15, 1–4. https://doi.org/10.1016/j.jrras.2022.05.018.

Lubin, J.H., Linet, M.S., Boice, J.D., Buckley, J., Conrath, S.M., Hatch, E.E., Kleinerman, R.A., Tarone, R.E., Wacholder, S., Robison, L.L., 1998. Case-control study of childhood acute lymphoblastic leukemia and residential radon exposure. J. Natl. Cancer Inst. 90 (4), 294–300. https://doi.org/10.1093/jnci/90.4.294.

Marsh, J.W., Bailey, M.R., 2013. A review of lung-to-blood absorption rates for radon progeny. Radiat. Protect. Dosim. 157 (4), 499–514. https://doi.org/10.1093/rpd/nct179.

Marsh, J.W., Birchall, A., 2000. Sensitivity analysis of the weighted equivalent lung dose per unit exposure from radon progeny. Radiat. Protect. Dosim. 87 (3), 167–178. https://doi.org/10.1093/oxfordjournals.rpd.a032993.

Marsh, J.W., Birchall, A., 2009. Uncertainty analysis of the absorbed dose to regions of the lung per unit exposure to radon progeny in a mine. Health Prot. Agency Rep. ISBN 978-0-85951-642-6.

Marsh, J.W., Bessa, Y., Birchall, A., Blanchardon, E., Hofmann, W., Noßke, D., Tomasek, L., 2008. Dosimetric models used in the Alpha-Risk Project to quantify exposure of uranium miners to radon gas and its progeny. Radiat. Protect. Dosim. 1–6. https://doi.org/10.1093/rpd/ncn119.

Marsh, J.W., Birchall, A., Davis, K., 2005. Comparative dosimetry in homes and mines: estimation of K-factors. Radioact. Environ. 7, 290–298. https://doi.org/10.1016/S1569-4860(04)07032-9.

Marsh, J.W., Birchall, A., Butterweck, G., Dorrian, M.D., Huet, C., Ortega, X., Reineking, A., Tymen, G., Schuler, Ch, Vargas, A., Vezzu, G., Wendt, J., 2002. Uncertainty analysis of the weighted equivalent lung dose per unit exposure to radon progeny in the home. Radiat. Protect. Dosim. 102 (3), 229–248. https://doi.org/10.1093/oxfordjournals.rpd.a006092.

Marsh, J.W., Blanchardon, E., Gregoratto, D., Hofmann, W., Karcher, K., Noßke, D., Tomasek, L., 2012. Dosimetric calculations for uranium miners for epidemiological studies. Radiat. Protect. Dosim. 1–13. https://doi.org/10.1093/rpd/ncr310.

Marsh, J.W., Harrison, J.D., Laurier, D., Blanchardon, E., Paquet, F., Tirmache, M., 2010. Dose conversion factors for radon: recent developments. Health Phys. 99 (4), 511–516. https://doi.org/10.1097/hp.0b013e3181d6bc19.

Marsh, J.W., 2022. Dosimetry Protocol for Miners and Millers [Unpublished Report]. United Kingdom Health Security Agency (UKHSA), Oxfordshire OX 11 0RQ, UK.

Mercer, R.R., Russell, M.L., Crapo, J.D., 1991. Radon dosimetry based on the depth distribution of nuclei in human and rat lungs. Health Phys. 61, 117–130. https://doi.org/10.1097/00004032-199107000-00013.

Miller, G., Inkret, W.C., Little, T.T., Martz, H.F., Schillaci, M.E., 2001. Bayesian prior probability distributions for internal dosimetry. Radiat. Protect. Dosim. 94 (4), 347–352. https://doi.org/10.1093/oxfordjournals.rpd.a006509.

Mirsch, J., Hintz, L., Maier, A., Fournier, C., Löbrich, M., 2020. An assessment of radiation doses from radon exposure using a mouse model system. Int. J. Radiat. Oncol. 108 (3), 770–778. https://doi.org/10.1016/j.ijrobp.2020.05.031.

Möhner, M., Gellisen, J., Marsh, J.W., Gregoratto, D., 2010. Occupational and diagnostic exposure to ionizing radiation and leukemia risk among German uranium miners. Health Phys. 99 (3), 314–321. https://doi.org/10.1097/HP.0b013e3181cd6536.

Möhner, M., Lindtner, M., Otten, H., Gille, H.G., 2006. Leukemia and exposure to ionizing radiation among German miners. Am. J. Ind. Med. 49, 238–248. https://doi.org/10.1002/ajim.20289.

Morgan, M.G., Henrion, M., 1990. Uncertainty: A Guide to Dealing with Uncertainty in Quantitative Risk and Policy Analysis. Cambridge University Press.

NCRP, 2009. Uncertainties in Internal Radiation Dose Assessment. NCRP Report 164. NCRP, Bethesda, MD.

Niinimaa, V., Cole, P., Mintz, S., Shephard, R.J., 1980. The switching point from nasal to oro-nasal breathing. Respir. Physiol. 42, 61–71. https://doi.org/10.1016/0034-5687(80)90104-8.

Niinimaa, V., Cole, P., Mintz, S., Shephard, R.J., 1981. Oronasal distribution of respiratory airflow. Respir. Physiol. 43, 69–75. https://doi.org/10.1016/0034-5687(81)90089-x.

Papenfuß, F., Maier, A., Sternkopf, S., Fournier, C., Kraft, G., Friedrich, T., 2023. Radon progeny measurements in a ventilated filter system to study respiratory-supported exposure. Sci. Rep. 13, 10792 https://doi.org/10.1038/s41598-023-37697-7.

Paquet, F., Bailey, M.R., Leggett, R.W., Harrison, J.D., 2016. Assessment and interpretation of internal doses: uncertainty and variability. Ann. ICRP 45 (1), 202–214. https://doi.org/10.1177/0146645316633595.

Postendörfer, J., 2001. Physical parameters and dose factors of the radon and thoron decay products. Radiat. Protect. Dosim. 94, 365–373. https://doi.org/10.1093/oxfordjournals.rpd.a006512.

Postendörfer, J., Reineking, A., 1999. Radon: characteristics in air and dose conversion factors. Health Phys. 76 (3), 300–305. https://doi.org/10.1097/00004032-199903000-00011.

Postendörfer, J., Zock, Ch, Reineking, A., 2000. Aerosol size distribution of the radon progeny in outdoor air. J. Environ. Radioact. 51 (1), 37–48. https://doi.org/10.1016/S0265-931X(00)00043-6.

Puncher, M., 2014a. Assessing the reliability of dose coefficients for ingestion and inhalation of ^{226}Ra and ^{90}Sr by members of the public. Radiat. Protect. Dosim. 158 (1), 8–21. https://doi.org/10.1093/rpd/nct188.

Puncher, M., 2014b. An assessment of the reliability of dose coefficients for intakes of radionuclides by members of the public. J. Radiol. Prot. 34, 625–643. https://doi.org/10.1088/0952-4746/34/3/625.

Puncher, M., Burt, G., 2013. The reliability of dose coefficients for inhalation and ingestion of uranium by members of the public. Radiat. Protect. Dosim. 157 (2), 242–254. https://doi.org/10.1093/rpd/nct134.

Puncher, M., Harrison, J.D., 2012a. Assessing the reliability of dose coefficients for inhaled and ingested radionuclides. J. Radiol. Prot. 32, 223–241. https://doi.org/10.1088/0952-4746/32/3/223.

Puncher, M., Harrison, J.D., 2012b. Uncertainty analysis of doses from ingestion of plutonium and americium. Radiat. Protect. Dosim. 148 (3), 284–296. https://doi.org/10.1093/rpd/ncr032.

Puncher, M., Bailey, M.R., Harrison, J.D., 2008. Uncertainty analysis of doses from inhalation of depleted uranium. Health Phys. 95 (3), 300–309. https://doi.org/10.1097/01.hp.0000314645.61534.b7.

Puncher, M., Birchall, A., Bull, R.K., 2012. A method for calculating Bayesian uncertainties on internal doses resulting from complex occupational exposures. Radiat. Protect. Dosim. 151 (2), 224–236. https://doi.org/10.1093/rpd/ncr475.

Puncher, M., Birchall, A., Bull, R.K., 2013. A Bayesian analysis of uncertainties on lung doses resulting from occupational exposures to uranium. Radiat. Protect. Dosim. 156 (2), 131–140. https://doi.org/10.1093/rpd/nct062.

Raaschou-Nielsen, O., 2008. Indoor radon and childhood leukemia. Radiat. Protect. Dosim. 132 (2), 175–181. https://doi.org/10.1093/rpd/ncn288.

Rericha, V., Kulich, M., Rericha, R., Shore, D.L., Sandler, D.P., 2006. Incidence of leukemia, lymphoma, and multiple myeloma in Czech uranium miners: a case-cohort study. Environ. Health Perspect. 114 (6), 818–822. https://doi.org/10.1289/ehp.8476.

Romano, S., Caresana, M., Curioni, A., Silari, M., 2019. RaDoM2: an improved radon dosimeter. J. Instrum. 14 (10), P10019 https://doi.org/10.1088/1748-0221/14/10/P10019.

Ruzer, L.S., Nero, A.V., Harley, N.H., 1995. Assessment of lung deposition and breathing rate of underground miners in Tadjikistan. Radiat. Protect. Dosim. 58, 261–268.

Sakoda, A., Ishimori, Y., Kanzaki, N., Tanaka, H., Kataoka, T., Mitsunobu, F., Yamaoka, K., 2021. Dosimetry of radon progeny deposited on skin in air and thermal water. J. Radiat. Res. 1–1 https://doi.org/10.1093/jrr/rrab030.

Schumann, R.R., Gundersen, L.C., 1996. Geologic and climatic controls on the radon emanation coefficient. Environ. Int. 22, 439–446. https://doi.org/10.1016/S0160-4120(96)00144-4.

Skubacz, K., Wołoszczuk, K., 2019. Size distribution of ambient and radioactive aerosols formed by short-lived radon progeny. J. Sustain. Min. 18, 61–66. https://doi.org/10.1016/j.jsm.2019.03.006.

Skubacz, K., Wołoszczuk, K., Grygier, A., Samolej, K., 2023. Influence of dose conversion factors and unattached fractions on radon risk assessment in operating and show underground mines. Int. J. Environ. Res. Publ. Health 20, 5482. https://doi.org/10.3390/ijerph20085482.

Steinbuch, M., Weinberg, C.R., Buckley, J.D., Robison, L.L., Sandler, D.P., 1999. Indoor residential radon exposure and risk of childhood acute myeloid leukemia. Br. J. Cancer 81 (5), 900–906. https://doi.org/10.1038/sj.bjc.6690784.

Tomasek, L., Malatova, I., 2006. Leukemia and Lymphoma Among Czech Uranium Miners. Paper Presented at the Second European IRPA Congress on Radiation Protection, Paris, France.

UNSCEAR, 2000. Sources, Effects and Risks of Ionizing Radiation: Volume 1: Report of the United Nations Scientific Committee on the Effects of Atomic Radiation to the General Assembly, vol. 2000. ISBN 92-1-142238-8.

Wang, Y., Sun, C., Zhang, L., Guo, Q., 2021. Optimized method for individual radon progeny measurement based on alpha spectrometry following the Wicke method. Radiat. Meas. 142, 1–8. https://doi.org/10.1016/j.radmeas.2021.106558.

Winkler-Heil, R., Hofmann, W., Marsh, J.W., Birchall, A., 2007. Comparison of radon lung dosimetry models for the estimation of dose uncertainties. Radiat. Protect. Dosim. 127, 1–4. https://doi.org/10.1093/rpd/ncm339.